Environmental Modelling and Software 183 (2025) 106243

Contents lists available at ScienceDirect

Environmental Modelling and Software

journal homepage: www.elsevier.com/locate/envsoft

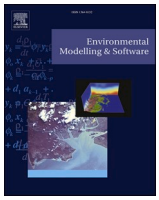

Hydro-geomorphological assessment of culvert vulnerability to flood-induced soil erosion using an ensemble modeling approach

Sourav Mukherjee [a,*], Sudhanshu Panda [b], Devendra M. Amatya [a], Mariana Dobre [c], John L. Campbell [d], Roger Lew [e], Peter Caldwell [f], Kelly Elder [g], Johnny M. Grace [h], Sherri L. Johnson [i]

[a] Center for Forested Wetlands Research, Southern Research Station, USDA Forest Service, 3734 Highway 402, Cordesville, SC, 29434, USA
[b] Institute of Environmental Spatial Analysis, University of North Georgia, 3820 Mundy Mill Road, Oakwood, GA, 30566, USA
[c] University of Idaho, Department of Soil and Water Systems, 875 Perimeter Drive, Moscow, ID, 83844, USA
[d] Northern Research Station, USDA Forest Service, Durham, NH, USA
[e] University of Idaho, Department of Virtual Technology and Design, 875 Perimeter Drive, Moscow, ID, 83844, USA
[f] Center for Integrated Forest Science, Southern Research Station, USDA Forest Service, 3160 Coweeta Lab Rd, Otto, NC, 28763, USA
[g] Rocky Mountain Research Station, USDA Forest Service, Fort Collins, CO, USA
[h] Center for Forest Watershed Research, Southern Research Station, USDA Forest Service, 1740 S. Martin, Tallahassee, FL, USA
[i] Pacific Northwest Research Station, USDA Forest Service, Corvallis, OR, USA

ARTICLE INFO

Keywords:
Soil erosion
Streambank erosion spatial vulnerability
Modified revised universal soil loss equation
Water erosion prediction project
Extreme precipitation and flooding
Automated geospatial-hydrology model
Stream crossings and culvert

ABSTRACT

Intense precipitation events pose growing threats to forest infrastructure causing flooding, and soil erosion and deposition, creating bottlenecks at road-stream crossing structures (RSCS). We describe a hillslope-scale ensemble hydro-geomorphological vulnerability assessment integrating geospatial Streambank Erosion Vulnerability Assessment (SBEVA), Modified Revised Soil Loss Equation (MRUSLE), and process-based Water Erosion Prediction Project (WEPP) model into an ensemble hydro-geomorphologic vulnerability index (EHVI) for USDA Forest Service (USFS) managed 194 road-culverts at the Hubbard Brook Experimental Forest (HBR-EF) in New Hampshire, USA. The results revealed that five and one culvert with diameters of 0.46m and 0.61m, respectively, have extreme EHVI values between 4 and 5, and fifteen and three culverts with diameters of 0.46m and 0.61m, respectively, have severe EHVI values between 3 and 4, some of which were previously identified as hydrologically vulnerable (undersized) to floods. This knowledge will inform USFS efforts to improve the resilience of the RSCS and protect aquatic habitats.

1. Introduction

Road stream crossing structures (RSCS), such as culverts and bridges, play a critical role in the forest road network by balancing resource management and traffic needs with aquatic habitat preservation (Cafferata and Cafferata, 2004; Keller and Sherar, 2003; Seddon et al., 2021). These RSCS may fail **catastrophically** when flood waters, caused by extreme precipitation events, exceed the hydraulic capacity of culverts and/or sediment and debris flow plug the culverts and damage bridges (Gillespie et al., 2014; Mukherjee et al., 2024; Truhlar et al., 2020). **Intense, short-duration rainfall events**, characterized by high precipitation rates and often associated with convective systems, pose a threat of intense floods (Amatya et al., 2021; Mukherjee et al., 2023; Mishra et al., 2022; Panda et al., 2022; Goodman et al., 2023). These "brutal floods," as dubbed by the National Oceanic and Atmospheric Administration and Drobot and Parker (2007), typically last between 2 and 6 h which exceeds the time of concentration and drainage capacity of catchments, especially for small head water streams. The short-lasting torrential flash floods (i.e., cloudburst floods) have now become a widespread and hazardous natural phenomenon in the world and are creating instant peril in mountain landscapes (Kuksina et al., 2017). The rapid influx of flood water results in **exceedingly high flow velocities**, triggering **widespread and severe stream bank and channel erosion**. Furthermore, the erosive power of these floods dislodges and transports sediment and debris of various sizes, significantly altering, channel morphology and water quality, blocking road-stream crossing structures

* Corresponding author.
E-mail address: sourav.mukherjee@usda.gov (S. Mukherjee).

https://doi.org/10.1016/j.envsoft.2024.106243
Received 10 July 2024; Received in revised form 12 September 2024; Accepted 7 October 2024
Available online 9 October 2024

and potentially harming aquatic habitats (Beilicci and Beilicci 2024). Reports of these events are widespread, and their intensity and frequency have increased in recent decades, impacting both experimental forest regions and national forest lands managed by the USDA Forest Service (Amatya et al., 2016; Gillespie et al., 2014; Glasser 2005).

Inadequately sized RSCS exacerbate flood risks, leading to structural failures, financial losses, and disruptions to stream connectivity that is essential for humans and aquatic organisms (Heredia et al., 2016). However, a more prevalent cause of culvert failure is the accumulation of sediment and/or debris at the culvert inlet (Xu et al., 2019). These sediment deposits create a bottleneck, restricting flow and potentially leading to catastrophic overtopping and eventually scouring the road during flood events (Furniss et al., 1998; Foltz et al., 2008; MacDonald and Coe, 2008; Muste and Xu, 2022; Panda et al., 2022). Notably, many culverts on USFS managed land are likely undersized for projected future flood conditions, highlighting the need for improved design considerations for flood resilience (Rasmussen et al., 2018; Amatya et al., 2021; Gillespie et al., 2014). Thus, it is critical to develop an efficient geomorphologic vulnerability assessment that aids in identifying culverts at risk of partial or full blockage from sediment deposition during flood events. The risk of culvert failure can be mitigated by adding an extra layer of safety in sizing, design, and restoration of culverts located in hydro-geomorphologically vulnerable areas (Furniss et al., 1997; Flanagan and Laflen, 1997; Furniss et al., 1998).

Streambank and gully erosion are major sources of soil loss and sediment delivery, amounting to hundreds of millions of tons annually across the U.S. (EPA, 2000; Poesen et al., 2003; NRCS, 2020; Shields et al., 1995; Cancienne et al., 2008; Langendoen and Simon, 2008; Wilson et al., 2022). Traditional empirical/conceptual erosion models, such as USLE, RUSLE, MUSLE, and RUSLE2, mainly account for sheet, rill, inter-rill, and to some extent gully erosion induced by surface flow (Risse et al., 1993; Panda et al., 2005; Borrelli et al., 2017; Tsegaye and Bharti, 2021; Panda et al., 2022; Panda et al., 2024; NRCS, 2020), but neglect the subsurface flow contributions to erosion processes like landslides and streambank erosion (Fox and Wilson, 2010).

In steep headwater catchments, the **hillslope area (upslope accumulated area)** is a primary factor influencing the stream channel sediment detachment and deposition downstream (Aksoy and Kavvas, 2005). This **hillslope-stream connectivity** reflects the interaction among key elements of the headwater landscape (topography, aspect, soil properties, and vegetation) and runoff along the hillslope gradient, which together determine the hydro-geomorphological vulnerability of RSCS during flood events (Jencso et al., 2009). Therefore, it is crucial to determine the hydro-geomorphological vulnerability at a hillslope scale. Additionally, **hillslope-stream** connectivity varies across space and can change over time and, forest management (such as harvesting) affects stream sediment yields, resulting directly from immediate erosion and sediment delivery from overland sources like high-gradient forest roads, especially during floods (McEachran et al., 2021; Pandey et al., 2016). To incorporate the effect of management and hillslope-stream connectivity dynamics on soil erosion potential, we used the **Water Erosion Prediction Project (WEPP)** (Nearing et al., 1989; Laflen et al., 1997) which is a process-based **continuous simulation model** and predicts not just the average soil loss, but the dynamic processes of soil erosion and deposition across the entire hillslope driven by precipitation and runoff (Lew et al., 2022; Dobre et al., 2022). **Process-based approach** offers significant advantages over traditional empirical methods as it can predict both the spatial and temporal variations of soil loss and deposition (Dobre et al., 2022; Lew et al., 2022; Costabile et al., 2024). Additionally, WEPP's broad applicability stems from its integration of process-based components that simulate surface and subsurface hydrology, water balance, plant growth, residue accumulation and decomposition, soil consolidation, and even stochastic weather generation, among other features that expand its usefulness.

Although there have been previous hydro-geomorphological assessments, there is a need for further research to better understand and incorporate the variability and interdependence of geomorphology dependent erosion processes and associated environmental factors, such as available water capacity in deeper soil layers, forest topography, soil characteristics, antecedent soil moisture, vegetation dynamics (Naipal et al., 2018), and climate change-induced extreme precipitation (Panda et al., 2022). To address this gap in knowledge, we used an Integrated Environmental Modeling (IEM) approach, inspired by contemporary problems demanding higher-order systems thinking and holistic solutions (EPA US Environmental Protection Agency, 2008; Jakeman and Letcher, 2003; Parker et al., 2002; Laniak et al., 2013; Raj et al., 2024). IEM concepts are relevant and useful for emerging issues like regional-scale spatial land-use management, climate change, and ecosystem services (Laniak et al., 2013; Panda et al., 2022 applied two geospatial watershed management models: the conceptual event-based modified RUSLE2 (MRUSLE) and the Streambank Erosion Spatial Vulnerability Assessment (SBEVA: Panda et al., 2022) to address these challenges. These are somewhat similar to one of the three methods described by Benjankar et al. (2013) and serve as practical geospatial decision-support systems for risk management.

An ensemble modeling approach that utilizes the event-based MRUSLE model, the geospatial SBEVA model, and the continuous simulation, process- and hillslope-based WEPP model is ideal for developing a comprehensive flood driven hydro-geomorphologic vulnerability assessment of culverts, including uncertainties, in small-forested headwater (and hillslope) catchments. While past studies have employed these models to evaluate hydro-geomorphologic vulnerability in watersheds (Dun et al., 2009; Panda et al., 2022; Shi et al., 2022; Dobre et al., 2022; Woznicki et al., 2020), this study presents a novel application by focusing on individual culvert vulnerability to flooding within its forested hillslope catchment. The main goal of this study was to assess the vulnerability of 194 culverts in the high gradient Hubbard Brook Experimental Forest (HBR-EF) in New Hampshire by creating an ensembled hydro-geomorphologic vulnerability index (EHVI) that integrates a SBEVA based stream-bank erosion vulnerability index with the annual average soil erosion estimates from the empirical/conceptual MRUSLE and process-based WEPP models.

The specific objectives of the study are to.

i) **Develop streambank erosion vulnerability maps using the SBEVA model and identify the culverts draining the hillslopes containing the hydro-geomorphologically vulnerable stream-bank areas.**
ii) **Estimate the total soil erosion at the inlet of the culverts using both the MRUSLE and WEPP models separately for the hillslope areas and validate the results against observed soil erosion data.**
iii) **Create flood hydro-geomorphologic vulnerability maps based on EHVI for the culverts by combining the total soil erosion potentials calculated using the MRUSLE and WEPP models with the streambank erosion vulnerability map developed using the SBEVA model.**
(iv) **Evaluate the performance of EHVI based on quantitative and qualitative assessment using observed erosion data and field survey results.**

2. Materials and methods

2.1. Study area

Our study was conducted at the US Forest Service (USFS) Hubbard Brook Experimental Forest (HBR-EF) of (3179 ha area, located within the White Mountain National Forest of central New Hampshire (43°56′N, 71°45′W). The HBR-EF has a humid continental climate, characterized by moderate winters and warm summers. Average monthly air temperatures range between −9 °C in January and 19 °C in July. Average annual precipitation is 1400 mm (ranging historically

from 970 mm to 1940 mm) and approximately one-third of precipitation falls as snow (Campbell et al., 2021). The HBR-EF watershed boundaries, elevation, stream and road networks, and culvert locations are shown in Fig. 1a. The hillslope boundaries upslope of each of the culvert inlets, are shown in Fig. 1b. In addition, a description of the study watersheds within the HBR-EF are provided in Table 1. The deciduous forest, evergreen forest, and mixed forest are the dominant land cover types, occupying 1492.5 ha (47.6%), 601 ha (19.2%), 1011 ha (32.2%) of the HBR-EF (3179 ha), respectively (Fig. S1).

2.2. Data and software

Watershed features, hydrometeorological, high resolution digital elevation model (DEM), soil, forest management, and culvert data were collected for the HBR-EF watersheds from various sources stated below. The following data were used in the development of automated geospatial-hydrology models SBEVA and MRUSLE model using ArcGIS Software by developing toolboxes available at GitHub (Panda (2024)). Fig. 2 demonstrates the methodology adopted in this study through a workflow diagram, and the description of variables, model application, and data sources are provided below and summarized in Table 2.

Table 1
Description of the gauged watersheds at the Hubbard Brook Experimental Forest (HBR-EF).

HBR-EF Watershed	Area (ha)	Slope (°)	Aspect	Elevation (m, a.m.s.l)
WS1	11.8	19.8	S 17° E	488–747
WS2	15.6	19.8	S 28° E	503–716
WS3	42.4	17.2	S 23° W	527–732
WS4	36.1	17	S 42° E	442–747
WS5	21.9	17.6	S 28° E	488–762
WS6	13.2	16.3	S 37° E	549–792
WS7	77.4	15.9	N 20° W	619–899
WS8	59.4	17.2	N 11° W	610–905
WS9	68.4	14.9	N 17° E	685–910

2.2.1. Watershed landscape data

LiDAR-based elevation data at 1-m resolution was obtained from the USDA Natural Resources Conservation Service Geospatial Data Gateway. The elevation data was resampled from 1-m to 5-m spatial resolution using bilinear interpolation. We developed a rust code using Topographic Optimization (TOPAZ) model to delineate the hillslopes in batches using the 5-m elevation data. The code is made available through GitHub (Lew (2024)). Land use and land cover information was obtained from the National Agriculture Imagery Program (NAIP)

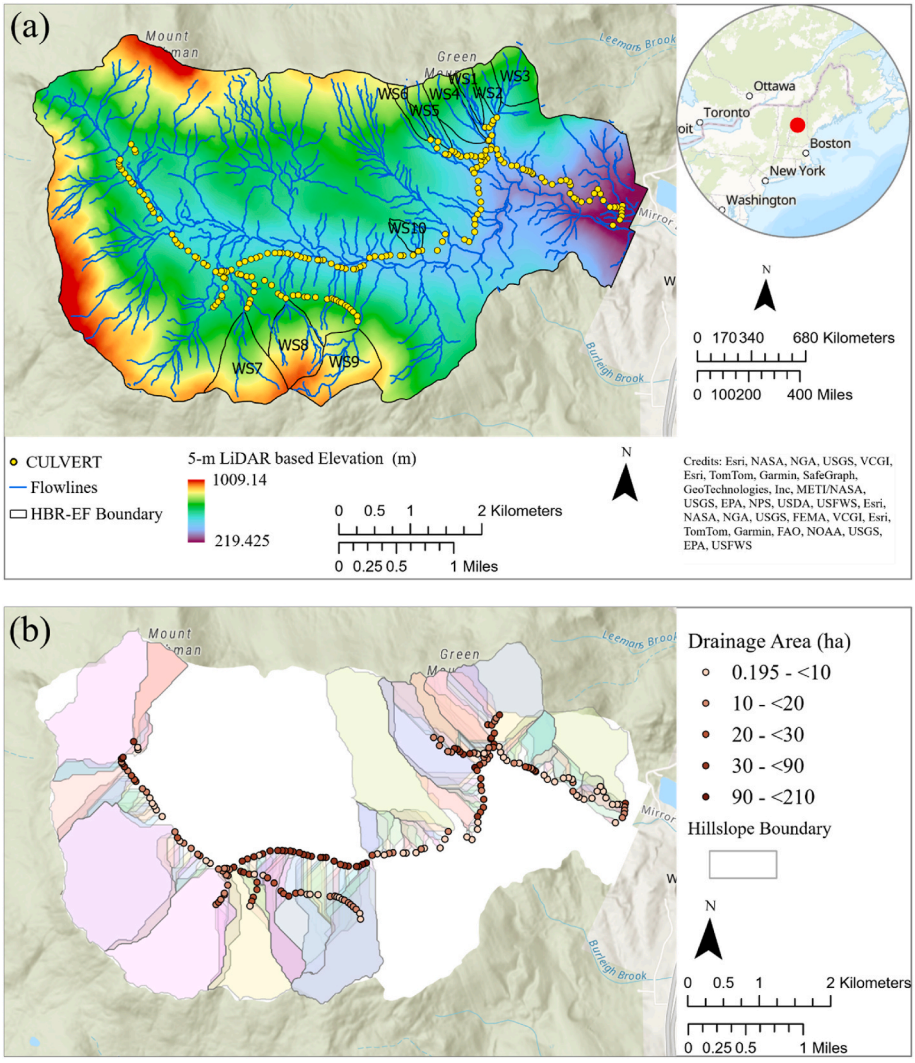

Fig. 1. Map of the Hubbard Brook Experimental Forest showing the (a) study area locations, watershed boundaries, culvert locations, and high-resolution LiDAR-based flowlines, and (b) hillslope boundaries and hillslope area draining into the culverts. Note that the flowlines are derived using 1-m resolution LiDAR elevation data.

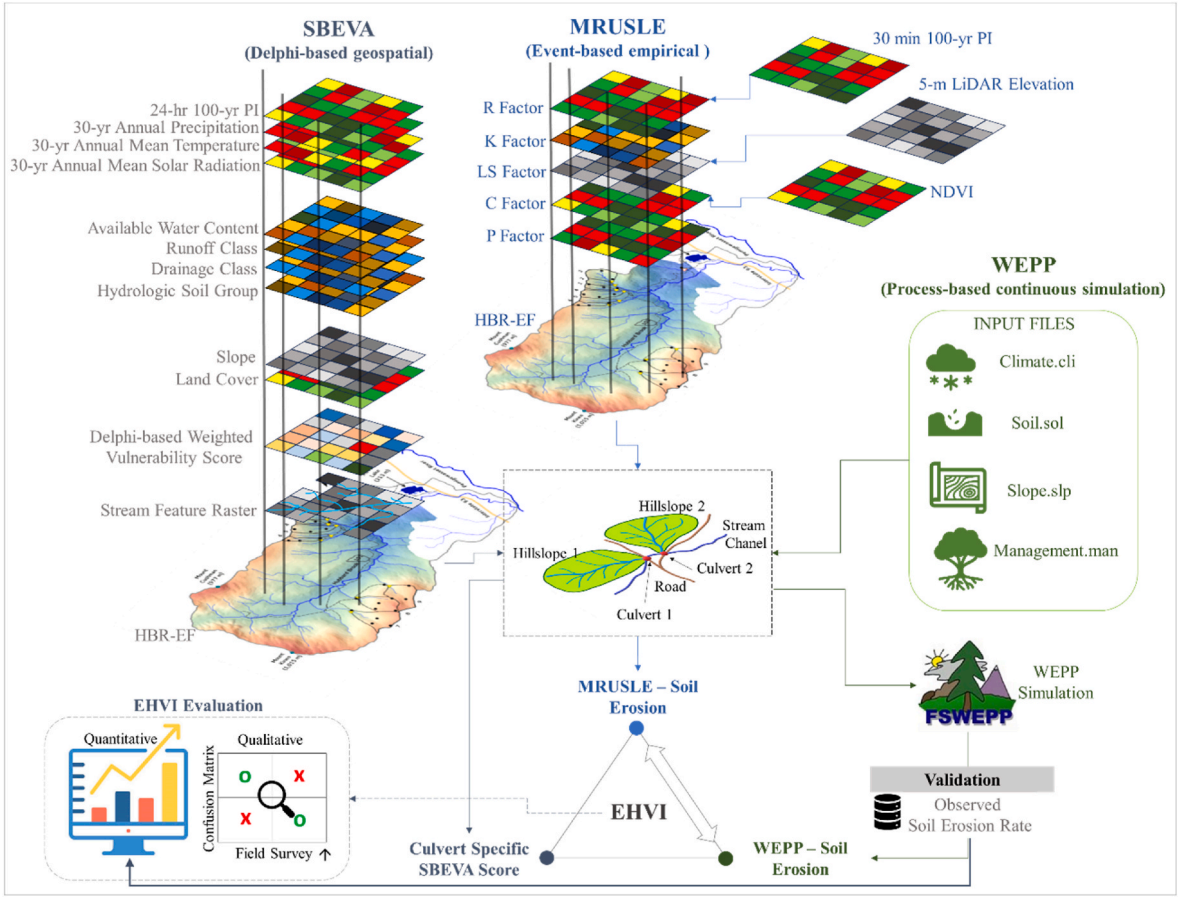

Fig. 2. Workflow diagram demonstrating the data and methodology used in the study.

land-use dataset available at 1-m spatial resolution from USDA Farm Service Agency. The NAIP acquires aerial imagery during the growing season in the continental United States. The red and near infrared bands were extracted from NAIP's imagery to calculate the Normalized Difference Vegetation Index (NDVI), which was used in the MRUSLE model development for pixel-scale erosion estimation.

2.2.2. Culvert data

Primary and secondary roads data were obtained from the Census Bureau's Topologically Integrated Geographic Encoding and Referencing (TIGER) database (Marx 1990), Enterprise Data Warehouse of the US Forest Service, and US Transit Roads for the HBR-EF (Mukherjee et al., 2024). The road network data from all three sources were further merged into one complete road network feature layer. The culvert database was developed from a field survey that recorded culvert location (latitude, longitude), diameter, construction material, and condition information for 194 culverts (Mukherjee et al., 2024).

2.2.3. Climate data

NOAA's interpolated 100-yr, 30-min and 24-hr precipitation intensity-duration-frequencies (PIDFs) were obtained from the NOAA Atlas-14's Precipitation Frequency Data Server (PFDS, Perica et al., 2015) although limited gauge specific such data were recently published by Mukherjee et al. (2023). The NOAA's Atlas-14 PI raster data were used in the SBEVA and MRUSLE models due to the small number of available USFS's onsite rain gauge stations. Long-term, 1991–2020 period (30-yr) annual average daily precipitation, mean temperature, and total clear-sky global shortwave radiation data were obtained from the Parameter-elevation Regressions on Independent Slopes Model (PRISM) available at 800-m spatial resolution from the PRISM climate group (Daly et al., 1997).

We used observed climate data for the period 1980–2023 in the WEPP model by combining observations from a rain gauge (RG01), and a weather station (HQMET), both managed by the USFS located within HBR-EF, and the gridded surface meteorological dataset from the University of Idaho (gridMET; Abatzoglou (2013)). Daily precipitation depth, storm duration, ratio of time to peak precipitation to storm duration, and ratio of maximum precipitation intensity to average precipitation intensity of storm events were obtained from USFS managed rain gauge number 1 (RG01) located within the HBR-EF at an elevation of 478 m a.m.s.l (Mukherjee et al., 2023). Minimum and maximum daily temperature, and solar radiation were obtained from the weather station located at HBR-EF headquarter (HQMET). Daily dew point temperature, and wind direction and magnitude were not available for the full period 1980–2023 (44 years) and therefore were obtained from the gridMET dataset. The gridMET data (4 km resolution) was extracted for the nearest Pinkham Notch, NH weather station located at 44.27N and −71.25W (latitude and longitude) coordinates, and at an elevation of 609 m a.m.s.l. The WEPP input data pre-processing, model automation, and runs were performed by developing and running python codes which are available publicly at Mukherjee (2024).

2.2.4. Soil data

Available soil water capacity (AWC) at deeper levels (weighted average value for 0–150 cm depth), soil drainage class, runoff class, hydrological soil group, and soil erodibility factor (K-factor) raster data were extracted from the SSURGO dataset available at 10-m spatial resolution from Web Soil Survey by USDA and NRCS. Observed soil erosion data were available for the WS1, WS5, and WS6 in the HBR-EF for the period 1980–2022 (USDA Forest Service, Northern Research Station,

Table 2
Description of variables, data sources and model applications used in the study.

Variable	Native Spatial Resolution	Temporal Resolution	Source	Used in
LiDAR Elevation	1-m	NA	US Department of Agriculture Natural Resources Conservation Service (USDA-NRCS)	SBEVA, MRUSLE, WEPP
Land Use Land Cover	1-m	NA	National Agriculture Imagery Program (NAIP)	SBEVA and MRUSLE
Road Network	NA	NA	Census Bureau's Topologically Integrated Geographic Encoding and Referencing (TIGER) database (available at https://datagateway.nrcs.usda.gov/), Enterprise Data Warehouse of US Forest Service (available at https://www.fs.usda.gov/about-agency/enterprise-data-warehouse), and US Transit Roads (available at https://www.bts.gov/maps)	SBEVA, MRUSLE, WEPP
Culvert data	NA	NA	USDA-FS	SBEVA, MRUSLE, WEPP
Observed erosion rate	WS1, WS5, and WS6	Sub-annual (Irregular intervals)	USDA-FS	Validation of WEPP and EHVI
Observed instantaneous streamflow	WS1, WS5, and WS6	5-min	USDA-FS	Validation of EHVI
30-min and 24-hr 100-yr Precipitation Intensity	0.00833333 by 0.00833333°	NA	NOAA-Atlas14	MRUSLE
30-yr average daily Precipitation	800-m	NA	Parameter-elevation Regressions on Independent Slopes Model (PRISM)	SBEVA
30-yr average daily mean Temperature	800-m	NA	Parameter-elevation Regressions on Independent Slopes Model (PRISM)	SBEVA
30-yr average daily total clear-sky global shortwave radiation	800-m	NA	Parameter-elevation Regressions on Independent Slopes Model (PRISM)	SBEVA
Daily dew point temperature, and wind direction and magnitude	NA	daily	gridded surface meteorological dataset from the University of Idaho (gridMET) from Pinkham Notch weather station.	WEPP
Daily precipitation, minimum and maximum daily temperature, and solar radiation	NA	daily	USDA-FS managed rain gauge, RG01, and weather station, HQMET.	WEPP
Available soil water capacity at deeper levels, soil drainage class, runoff class, hydrological soil group, and soil erodibility factor (K-factor)	10-m	NA	SURGO data from Web Soil Survey by USDA and NRCS	SBEVA, MRUSLE, and WEPP

NA: Not Applicable.

2024) which were used in the validation of the WEPP outputs. Each year the sediment that collects in the stilling basin behind the v-notch weir is measured, excavated, sampled, dried, and weighed for the watersheds. Oven-dry weights are then calculated for all of the sediment removed from the basin and extrapolated back over the watershed as mass of soil material lost per unit area (Martin and Hornbeck, 1994).

These data were gathered as part of the Hubbard Brook Ecosystem Study (HBES). The HBES is a collaborative effort at the Hubbard Brook Experimental Forest, which is operated and maintained by the USDA Forest Service, Northern Research Station. All raster datasets were resampled to 5-m spatial resolution for consistency with the resampled 5-m LiDAR based elevation dataset stated above.

2.3. SBEVA model development

We used the SBEVA model (updated upon Panda et al., 2022) to identify stream segments that are vulnerable to erosion at culvert inlets and outlets using ten geospatial variables: (1–3) the PRISM's annual average (1) precipitation, (2) temperature, and (3) incoming solar radiation raster (900 m), (4) NOAA-Atlas14's 24-hr 100-yr PIDF raster (https://hdsc.nws.noaa.gov/hdsc/pfds/) available at a spatial resolution of 900 m, (5–8) SSURGO's (5) available soil water capacity at deeper levels, (6) drainage class, (7) runoff class, and (8) hydrological soil group raster (10-m), (9) classified NAIP imagery raster (1 m) for land cover classification, and (10) slope derived from LiDAR-based DEM raster (5-m) as shown in Table 2.

Each raster was pan-sharpened to achieve a consistent spatial resolution of 5-m using ArcGIS software. These 5-m spatial resolution rasters were then reclassified into an equal number of categories and each category was assigned a unitless score. The scoring was assigned based on the geometric distribution of the dataset across pixels within the HBR-EF boundary and erosion potential along the stream bank. The grouping was based on the geometric distribution, which reflects the frequency of occurrence of each score across the entire area. With this method, areas with more common scores were grouped together into similar vulnerability classes. The pixels with higher precipitation were assigned a higher vulnerability score. Similarly, land-use was reclassified by its potential for streambank erosion: dense forest on the streambank (having a lower erosion potential) was assigned the lowest score and bare soil on the stream bank was assigned the highest score. The DEM raster was converted into a slope raster and classified following the methodology described previously. The lowest slope degree range was assigned the lowest streambank erosion vulnerability score and vice-versa. The SSURGO raster was also reclassified to create several streambank erosion vulnerability rasters, with five contributing soil characteristics, including available soil water capacity in deeper soil layers, soil hydrologic group, drainage class, and runoff class. Each of the characteristics was classified with a vulnerability score: the lowest score was assigned to the soil with the lowest potential for erosion vulnerability, and the highest score was assigned to the soil with the highest potential for erosion vulnerability.

Once all the spatial factors contributing to the streambank erosion process were classified, they were assimilated through a Weighted Sum tool available in ArcGIS following the widely used Delphi method weight assignment process (Panda et al., 2022; MacMillan and Marshall, 2006). The Delphi method-based weight assignment process was used to assign percentile weights to each environmental factor during the Weighted Sum application. The reclassified data were given weights that determined their potential for influencing erosion vulnerability. Each soil runoff class was assigned a weighted score of 10%, while land-use, slope gradient, and 24-hr 100-yr extreme precipitation were assigned scores of 16%, 18%, and 19%, respectively. The entire process was carried out for the entire stream network. The authors of this manuscript along with professional experts from USFS (Southern Research Station);

University of Georgia, GA; and University of Idaho were asked to provide their opinion on vulnerability weight scales for all ten layers used in the model development.

The SBEVA analyses were conducted within the 10-m buffer of the entire stream network. The result of the Weighted Sum was aggregated over the pixels within this 10-m buffer zone within individual hillslopes yielding a cumulative SBEVA score for each culvert draining a given hillslope. It is important to note that 23 out 194 hillslopes are not connected to stream channels and were thus excluded from the calculation of the cumulative SBEVA scores.

2.4. MRUSLE model development

The RUSLE2 model (referred to as MRUSLE) includes six environmental factors (Renard et al., 1994; Renard et al., 2017; Benavidez et al., 2018) as model parameters shown in Eq. (1) below:

$$A_i = R_i \times K_i \times L\,S_i \times C_i \times P_i \quad (1)$$

where, A_i = soil-erosion rate (t ha^{-1} yr^{-1}), R_i = rainfall erosivity factor evaluates the effect of rainfall impact in the form of kinetic energy (*KE*), LS_i = slope length and steepness factor, K_i = soil erodibility factor (obtained from SSURGO database), C_i = crop management factor (developed with land-use map reclassification), and P_i = conservation practice factor (a constant value for a managed watershed) for the ith pixel. Following Fernandez et al. (2003), a P factor value of 1 was used in the study.

The R-factor was developed separately using NOAA-Atlas14 30-min 100-yr precipitation intensity (PI_{30}) raster given as,

$$R_i = KE_i \times PI_{30i} \quad (2)$$

Panda et al. (2022) modified the RUSLE model over Wischmeier and Smith (1978) who suggested a limited constant value of $KE = 0.283$ MJ ha^{-1} hr^{-1} mm^{-1} for rainfall intensities (PI_{30i}) exceeding 76 mm/h (Yin et al., 2017) or

$$KE_i = 0.119 + 0.0873 \times log_{10}(PI_{30i}), PI_{30i} \leq 76\ mm\ /\ hr \quad (3)$$

where, PI_{30i} = 30-min rainfall intensity for a 100-yr storm at the ith pixel.

The K-factor raster was extracted from the SSURGO dataset. Values in the SSURGO database are presented in U.S. customary units (ton ac hr 100^{-1} ac^{-1} ft^{-1} tonf^{-1} in^{-1}), ranging from 0 to 0.64, with higher values reflecting greater erodibility (Renard, 1997; Woznicki et al., 2020). In SI units, K ranges from 0 to 0.08 t ha hr ha^{-1} MJ^{-1} mm^{-1}.

The LS factor was developed by Wischmeier and Smith (1957) given as,

$$LS_i = L_i \times S_i \quad (4)$$

where, $L_i = \left(\frac{\lambda}{\psi}\right)^m$, λ is flow path length (in m), λ = *Flow accummulation* × *cell size*, and $\psi = 22.13$ (in SI units).

The C-factor was estimated using a non-linear function of normalized difference vegetation index (NDVI)-based formula (Eq. (5)) developed by Van der Knijff et al. (2000) using an exponential decay relationship between NDVI and C factor given as,

$$C_i = e^{\left(-\alpha\left(NDVI_i/\beta - NDVI_i\right)\right)} \quad (5)$$

where, $\alpha = 2$, and $\beta = 1$ (Van der Knijff et al., 2000), and the $NDVI_i$ was calculated from reflectance measurements in the red (R) and near infrared bands (provided by the National Agriculture Imagery Program) for the ith pixel using, $NDVI_i = (NIR_i - R_i)/(NIR_i + R_i)$. The MRSULE analysis excludes lands that are considered non-erodible (for example the NLCD open water).

2.5. WEPP model development

The Watershed Erosion Prediction Project (WEPP) is a physical-based model developed by a consortium of US government agencies including the Agricultural Research Service, Soil Conservation Service, US Forest Service and the Bureau of Land Management (Laflen et al., 1991; Flanagan and Nearing, 1995; Srivastava et al., 2019; Lew et al., 2022; Dobre et al., 2022). WEPP has been widely used for hillslope erosion prediction in the US and internationally (Laflen et al., 1991). It focuses on understanding and quantifying the key mechanisms of water erosion, including human influences and incorporates various processes, such as erosional, hydrological, plant growth and residue, water use, hydraulic, and soil processes (Laflen et al., 1991). The ability of WEPP to accurately predict where detachment and deposition will occur is useful in establishing appropriate conservation or management practices.

WEPP integrates a hydrology component based on a modified Green-Ampt infiltration equation and solutions of the kinematic wave equations. It includes processes like snow accumulation and melt, deep percolation of soil water, and subsurface lateral flow. The model incorporates a plant growth component that responds to changing environmental conditions such as soil moisture, rainfall, temperature, and solar radiation. Residue decomposition is also modeled based on site-specific soil and climate conditions. WEPP uses a stochastic weather generator (CLIGEN) to generate long-term daily weather values based on monthly and annual statistics of various weather parameters recorded at weather stations across the U.S. The model also allows the incorporation of specific daily weather parameters from gridded national weather products such as PRISM, Daymet, gridMET, and NEXRAD in conjunction with parameters generated by the CLIGEN model. This methodology enables users to run both historic simulations and long-term stochastic simulations (e.g., 100 years) with the model. Model outputs include daily soil evaporation, plant transpiration, runoff, subsurface lateral flow, baseflow, deep percolation, snow accumulation and melt, the soil water balance, and sediment yield for each hillslope, channel, and at the watershed outlet.

In this study, the hillslope version of WEPP was used to simulate average annual estimates of runoff and erosion at a hillslope scale draining into individual culverts. The WEPP hillslope profile erosion model uses a steady-state sediment continuity equation to describe the movement of sediment in a rill given by (Foster et al., 1995),

$$\frac{dG}{dx} = D_f + D_i \quad (6)$$

where x = distance downslope (in m), G = sediment load (in kg/s/m), D_i = interrill sediment delivery to the rill (in kg/s/m^2), and D_f = rill erosion rate (in kg/s/m^2). Interrill sediment delivery, D_i, is assumed to be independent of x, and is always positive. Rill erosion, D_f, is positive for detachment and negative for deposition. For model calculations, both D_f and D_i are computed on a per-rill area basis. Consequently, G is solved on a per-unit rill width basis. A more comprehensive explanation of the governing equations used in the WEPP hillslope profile erosion model is provided in Foster et al. (1995).

Hillslopes were delineated for each culvert by tracing the upslope areas of the culvert inlet points separately using 5-m LiDAR elevation data for the HBR-EF (Fig. 1b). **WEPP requires four main types of input data files: (1) climate, (2) slope, (3) soil, and (4) crop/management.** For each hillslope, **daily observed climate data was obtained by combining meteorological data from the RG01, HQMET station (managed by USDA-FS) and gridMET data from the Pinkham Notch, NH station for the period, 1980–2023 (see Method section). Slope data for each hillslope was generated using the 5-m LiDAR elevation dataset. Soil data was derived from the SSURGO dataset, and management data was derived using the National Land Cover Dataset of HBR-EF (Table 2).** The specific slope, soil, climate, and

landcover/management value was assigned to each hillslope (Renschler, 2003; Flanagan et al., 2013)

The model simulated runoff and snowmelt response to rainstorm or snow events identified based on observed daily climate data for the 44-yr period (1980–2023). WEPP calculated soil loss, sediment deposition, off-site sediment delivery, and enrichment of runoff produced by rainfall or snowmelt. WEPP calculated average values for erosion processes like detachment, deposition, sediment delivery, and enrichment for each hillslope separately for the simulation period. These averages were determined by dividing the total values by the chosen simulation years (44 years) to obtain the annual average erosion rates per hillslope discharged as sediment to the hillslope outlet, which is the culvert inlet.

The uncertainties associated with the simulation results of WEPP were assessed against the observed erosion data available for three watersheds W1, W5, and W6 in the HBR-EF for 1980–2022 period. The observed soil loss data was not available for specific calendar or water years. Therefore, we used the WEPP simulated event by event erosion rates by matching the time-interval to that of the observed record and then compared the average erosion rates for the 1980–2022 period. The uncertainty was analyzed using a percentage bias estimated as, PB (%) = [(WEPP – Obs.)/Obs.] x 100.

2.6. Estimation and evaluation of ensemble hydro-geomorphologic vulnerability index (EHVI)

The ensemble approach can provide a more wholistic estimate of soil erosion vulnerability, reducing reliance on any specific model's assumptions. Therefore, in this study, an ensemble hydro-geomorphologic vulnerability index (EHVI) was calculated for each of the 194 culverts draining the hillslopes by aggregating (averaging) the hillslope-based vulnerability classes obtained from the SBEVA, MRUSLE, and WEPP models.

The pixel based cumulative SBEVA scores were grouped into five vulnerability classes. Quantile classification in ArcGIS was used to distribute vulnerability classes into five groups. This method handles the issue where certain class ranges cover a broad value range, while other classes have a very narrow range. The lower cumulative SBEVA scores were assigned a vulnerability class 1, and the higher cumulative SBEVA scores were assigned a vulnerability class 5. Similarly, erosion rates for each pixel obtained from the MRUSLE model were averaged across hillslopes and multiplied by the hillslope area to obtain the total annual average erosion for each of the 194 culverts draining the hillslopes. The resulting MRUSLE total annual average erosion magnitudes are categorized into five vulnerability classes based on the quantiles. The WEPP model simulated annual erosion rates per drainage area for individual hillslopes were multiplied by the hillslope drainage area to obtain the total annual average erosion, which were then grouped into 5 similar vulnerability classes. The distribution of total erosion across the vulnerability classes were kept consistent between MRUSLE and WEPP. **Finally, the vulnerability classes (1 to 5) corresponding to the SBEVA, MRUSLE, and WEPP models were aggregated by averaging to obtain the EHVI for all 194 culverts. The EHVI** creates a holistic picture of erosion dynamics transported from upland hillslope and streambanks to the culvert inlet, addressing both short-term event-based and long-term hydro-geomorphologic vulnerability.

The EHVI was evaluated (or validated) both quantitively and qualitatively as described below.

(i) Quantitative Evaluation:

A quantitative evaluation of EHVI was performed against observed erosion and flow data, which is available for WS1, WS5, and WS6. We derived a GEV distribution using Extreme Value Analysis (EVA; Coles et al., 2001) and the annual time series of observed erosion data to estimate the return values of annual total erosion rates and peak flow for specific non-exceedance probabilities corresponding to 25-year, 50-year and 100-year return intervals. It is reasonable to assume that the distribution of annual total erosion rates may not necessarily follow the same extreme tail behavior as peak flows. Therefore, further statistical testing to check for the goodness-of-fit to GEV distribution is necessary. The goodness of fit to the GEV distribution was determined using the Kolmogorov-Smirnov test (refer to Massey (1951) for methods). If the p-value from the Kolmogorov-Smirnov test is high (typically above 0.05), it suggests that the data follows the GEV distribution (Massey, 1951). Once the time-series show a good fit to the GEV distribution, probability density functions and 25-year, 50-year, and 100-year return values of the annual total erosion rates and peak flow were calculated and compared across the watersheds (WS1, WS5 and WS6), and with the EHVI values for the culverts draining these watersheds.

The GEV is a three-parameter distribution comprised of the location (μ), scale (σ), and shape (ε) parameters whose theoretical cumulative distribution function is given as (Coles et al., 2001),

$$F_{GEV}(x|\mu,\sigma,\varepsilon) = exp\left[-\left(1+\frac{\varepsilon}{\sigma}(x-\mu)\right)^{-1/\varepsilon}\right], \mu \in R, \sigma > 0, \varepsilon \neq 0 \quad (7)$$

The p-quantile of the GEV distribution is then estimated as,

$$q_p = \left[\left(-\frac{1}{\ln(1-p)}\right)^{\varepsilon} - 1\right] \times \frac{\sigma}{\varepsilon} + \mu, (\varepsilon \neq 0) \quad (8)$$

where, (1-p) is the non-exceedance probability.

(ii) Qualitative Evaluation:

Qualitative evaluation of EHVI was performed based on field validation survey of a randomly selected subset of culverts followed by estimation of Accuracy and F1 score metrics based on confusion matrix depicted in Fig. 3. A Confusion matrix is commonly used to visualize the performance of a classification algorithm (Bagwan and Gavali, 2021). In this study, the observations from the field survey (actual conditions) were qualitatively compared to the EHVI values (predicted condition) which was finally transformed to a confusion matrix.

The Accuracy metric simply measures how often the classifier makes a correct prediction where.

$$Accuracy\ (\%) = \frac{TP + TN}{(TP + TN + FP + FN)} \times 100 \quad (9)$$

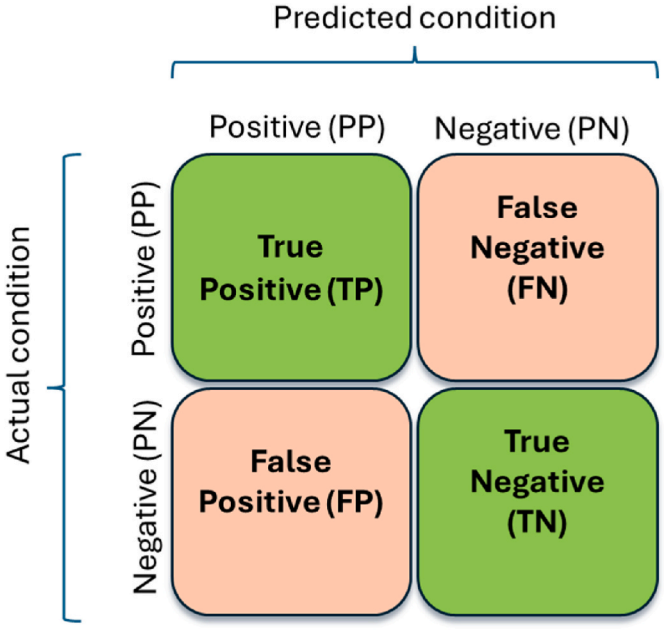

Fig. 3. Description of a confusion matrix.

The F1 score is a measure of a test's accuracy, considering both precision and recall. It's particularly useful when balance the trade-off between false positives and false negatives is crucial for decision making. F1 score can be calculated using a confusion matrix as depicted in Fig. 3. F1 score metric is calculated as a harmonic mean of precision and recall as shown below.

$$F1\ score = \frac{2 \times (Precision \times Recall)}{(Precision + Recall)} \quad (10)$$

where, precision is the ratio of true positives to the sum of true positives and false positives given as, $Precision = \frac{TP}{(TP+FP)}$, and recall is the ratio of true positives to the sum of true positives and false negatives given as, $Recall = \frac{TP}{(TP+FN)}$. Although the F1-score is not as intuitive as accuracy, it is useful in measuring how precise and robust the classifier is.

3. Results

3.1. SVEBA model outputs

The input variable rasters for the HBR-EF superimposed in the SBEVA model are shown in Fig. S2. The climate variable rasters for the 24-hr 100-yr PI range from 158 to 182 mm/h in magnitude, 30-yr average precipitation range from 1282 to 1582 mm, 30-yr average temperature range from 3.9 to 6.6 °C, and 30-yr average daily total clear-sky global shortwave radiation range from 19 to 20 MJ/m^2/day. The soil-property.

rasters derived from the SSURGO dataset lack heterogeneity. About 97% of the HBR-EF shows available soil water capacity ranging between 0.196 and 0.21, medium runoff class, well drained drainage class, and is characterized by a hydrologic soil group C. The slope raster indicates substantially varying slope, which is expected in the small high gradient headwater forested watersheds in the HBR-EF.

Fig. 4 shows the weighted aggregated (sum) SBEVA scores for pixels along the stream channel with a 10-m buffer zone, and the cumulative SBEVA score for the hillslopes, specific to their downstream road culvert locations, in the HBR-EF. The weighted aggregated SBEVA scores for pixels along the stream channel range from 1.3 to over 2.25. Areas with higher 30-yr annual average precipitation and more intense storms indicated by the 24-hr 100-yr PI show greater weighted SBEVA scores (Fig. S2). The western side of the HBR-EF shows relatively higher SBEVA scores (between 1.8 and 2.25).

The cumulative SBEVA scores across the hillslopes range from 1 to 415000. The hillslope cumulative SBEVA scores specific to the 194 culverts indicate that only 2 culverts are located in areas representing class 5 vulnerability, indicating them as the most susceptible to erosion hazard, 17 culverts are located in areas of class 4 vulnerability, 48 culverts are located in areas of class 3 vulnerability, 58 culverts are located in areas of class 2 vulnerability, and 46 culverts are located in areas of class 1 vulnerability indicating the least susceptibility to erosion hazard.

3.2. MRUSLE based soil erosion potential

The potential annual erosion rates obtained from the MRUSLE model for each pixel and for the specific hillslopes draining into the culverts within the HBR-EF is presented in Fig. 5. Fig. S3 shows the rainfall erosivity factor (R), soil erodibility factor (K), slope length and steepness factor (LS), and crop management factor (C) raster superimposed in the MRUSLE model. The maps in Fig. S3 indicate that except for the K factor, all other factors of the MRUSLE model show considerable spatial heterogeneity.

The hillslope averages of total erosion range from 0 to 1.5 t/yr across the 194 hillslopes with an average of 0.11 t/yr (Fig. 5b). Based on the total annual soil erosion rate for the hillslopes, the erosion rates, potentially discharges as sediment, were categorized into five vulnerability classes: class-1 (0–0.05), class-2 (0.05–0.1), class-3 (0.1–0.3), class-4 (0.3–0.6), class-5 (0.6–1.5), t/yr (Fig. 5b).

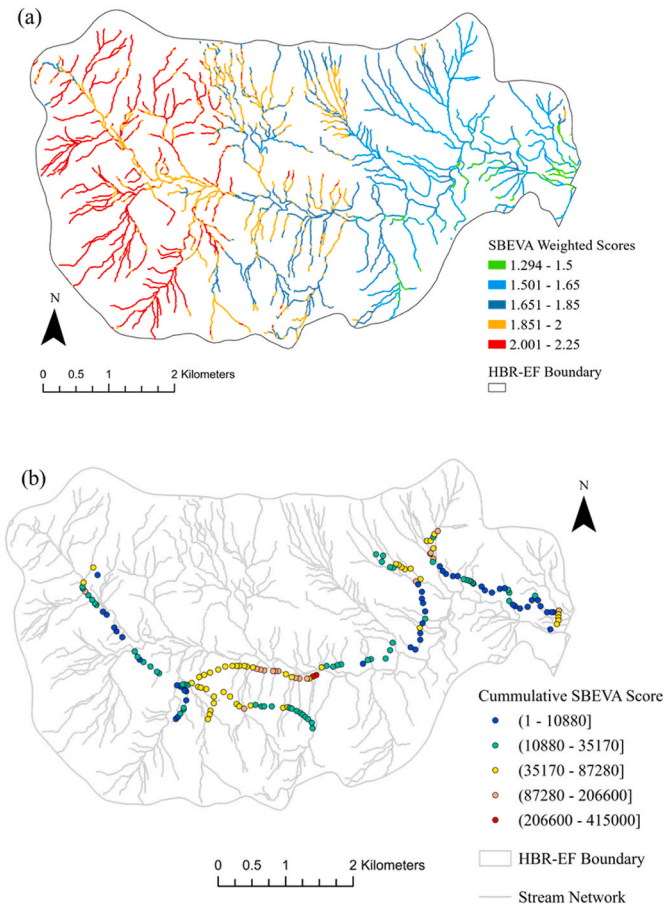

Fig. 4. Stream bank erosion vulnerability maps showing the (a) weighted SBEVA score for the 10-m buffer area of the stream channel, and (b) hillslope cumulative SBEVA scores for the HBR-EF developed using the SBEVA model.

3.3. WEPP based soil erosion potential

The WEPP simulation of total erosion rates calculated over a 44-year period (1980–2023) for 194 hillslope areas draining into the culverts are shown in Fig. 6. The results indicate that most of the hillslope areas draining into these culverts have low to moderate soil erosion rates. The average WEPP simulated total soil erosion across all hillslope areas range from 0 to 16 t/yr, with a mean value of 0.45 t/yr. Based on the total soil erosion, the HBR-EF has been categorized into five vulnerability classes (keeping it consistent with the class distribution applied for total erosion obtained from MRUSLE): class-1 (0–0.05), class-2 (0.05–0.1), class-3 (0.1–0.3), class-4 (0.3–0.6), class-5 (>0.6 t/yr (Fig. 6).

The WEPP model simulated a relatively higher average annual runoff of 43 mm/yr due to snowmelt. The WEPP simulated average annual runoff generated by rainfall is 15 mm/yr. The shortest and longest length of the hillslopes is 66 m and 2591 m. The total erosion for each of the individual hillslopes shows a considerable positive correlation with the drainage area of the hillslopes, as indicated by Pearson correlation coefficients of 0.54, respectively (Fig. S4) which would be as expected.

Based on the results of the uncertainty analysis, WEPP slightly underestimated the average annual erosion rate in WS1, and overestimated it in WS5, and WS6 as shown in Table 3. The WEPP simulated average annual erosion rate for the hillslope draining into the WS1 outlet was 33 kg/ha/yr or about 13% less than the average annual erosion rate of 38 kg/ha/yr observed at WS1, 52 kg/ha/yr or about 53%

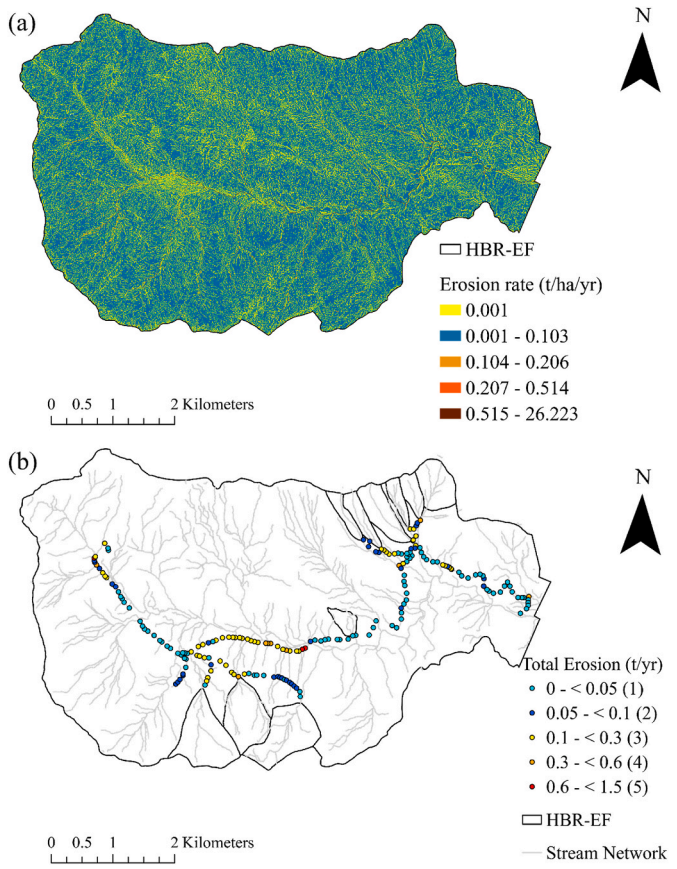

Fig. 5. Spatial map for the HBR-EF showing (a) pixel-based soil erosion rates calculated using the MRUSLE methodology, and (b) total erosion specific to the culverts. Note that in (b), the vulnerability classes are shown in parenthesis.

greater than the 34 kg/ha/yr erosion rate for WS5, and 30 kg/ha/yr or about 108% greater than the 14.4 kg/ha/yr for WS6 during the period 1980–2022.

3.4. Ensemble hydro-geomorphologic vulnerability of culverts

The distribution of total erosion at the 194 culverts obtained from MRUSLE, and WEPP and their ratios with respect to hillslope drainage area are shown in Fig. S5. The hillslope drainage area was binned based on the 0–25, 25–50, 50–75, and 75–100 percentile values. The ratio between total erosion obtained from the WEPP and the MRUSLE model show substantially increasing trend with increasing hillslope drainage area. The vulnerability class of EHVI for specific culvert diameters were compared with those obtained from the SBEVA, MRUSLE, and WEPP models (Fig. 7). The mean EHVI was greatest for the 1.83 m culverts, and lowest for the 0.46 and 0.61 m culverts. Relatively higher mean EHVI (>3) in areas draining into the greater diameter culverts (≥0.76 m), they are likely less vulnerable due to their capability to carry larger sediment loads.

Fig. 8 below shows the spatial map of culvert location and diameter, and EHVI for each culvert calculated as the average of the vulnerability class of SBEVA, MRSULE, and WEPP along with the culvert diameter (Fig. 8a and b). The EHVI values vary between 1 (lowest vulnerability) and 5 (highest vulnerability), averaging 2.23 for all 194 culverts. There are 43 (22.2% of 194 culverts) culverts whose EHVI value is between 3 and 4 and 16 (8.2%) culverts with EHVI value between 4 and 5. One culvert with 0.38 m diameter show EHVI value of 3. Out of the 43 culverts with an EHVI between 3 and 4, fifteen (7.7%) have a diameter of 0.46 m, three (1.5%) have diameter of 0.61 m, two (1%) have a diameter of 0.76 m, and three (1.5%) have a diameter of 0.91 m (Fig. 8c). It is important to note that five (2.6%), and one (0.5%) culvert with diameter 0.46 m and 0.61 m have EHVI value between 4 and 5. About 24.7% (18.6%) of the 194 culverts that are 0.46 m in diameter are in relatively lower vulnerability areas indicated by EHVI values between 1 and 2 (0 and 1).

3.5. Evaluation of EHVI

Fig. 9, S6, and S7, and Table S1 show the results of the quantitative and qualitative evaluation of EHVI. GEV distribution is found to be a statistically good fit as suggested by the results of goodness-of-fit test (at 0.05 significance level) using the Kolmogorov Smirnov test statistics and *p*-values. The *p*-values for the WS1, WS5, and WS6 are found to be 0.97, 0. 99, and 0.62 (>0.05), respectively. The EHVI correlates very well with the 25-year, 50-year and 100-year return values which offer insights into the potential erosion rates that can be expected on an average once in over a 25-year, 50-year and 100-year period, respectively. WS5 had the highest peak, and the highest 25-yr, 50-yr and 100-yr erosion rates, followed by WS1 and WS6 (Fig. 9a–b, and Fig. S6) indicating extreme erosion events are more likely in WS5 compared to WS1, and WS6. The WS5 also exhibits the highest annual peak discharge over the period 1980–2022 (Fig. S7). These results align with the EHVI values, which are highest for WS5 and lowest for WS6. The results indicate that EHVI exhibits a promising performance in capturing the extremes or low exceedance probability events.

The results of the qualitative evaluation of EHVI through a post-analysis field validation survey of culvert conditions are demonstrated in Fig. 9(c–e) and Table S1. The results include the photographs of the upstream, inlet, outlet, and downstream sections of randomly selected culverts to demonstrate the actual field conditions. The accuracy of EHVI was evaluated by feeding this information into the confusion matrix and by calculating widely used metrics, the accuracy metric, precision, recall and F1 score. Our findings revealed that the EHVI identified the vulnerable culverts with an accuracy of 75%. EHVI showed a precision of 0.8 which means that EHVI correctly predicted 80% of the hydro-geomorphologically vulnerable culverts. This indicates that EHVI has a high accuracy in predicting positive instances, with a low rate of false positives. EHVI showed a recall of 0.73 which means that it correctly identified 73% of all hydro-geomorphologically vulnerable culverts. This also indicates that EHVI is reliable at capturing most of the positive instances, though it misses some. Finally, EHVI showed a F1 score of 0.76 that EHVI maintains a good balance between precision and recall, effectively managing both false positives and false negatives. This indicates a good overall performance of EHVI in identifying the vulnerable culverts in this forest region.

While EHVI does not provide absolute vulnerability based on on-site physical conditions of the culverts, these results suggest that it serves as an effective off-site indicator that ranks vulnerability of culverts relative to one another, providing a basis for prioritizing the resources.

4. Discussion and limitations

The western side of the HBR-EF show relatively higher SBEVA scores mainly dominated by higher 30-yr annual average precipitation and more intense storms. The higher SBEVA scores indicate relatively higher potential for stream bank erosion and thereby a higher potential of sediment deposition into the downstream culverts. The soil properties did not play a significant role in determining the variability of the SBEVA scores because of the lack of spatial variability of SSURGO soil data for most of the area.

The results from the MRUSLE model indicate low levels of erosion potential of hillslopes draining into the culverts in the HBR-EF which is mainly due to the dominance of deciduous, evergreen, and mixed forest cover. These erosion rates are also consistent with the findings of Woznicki et al. (2020) for the HBR-EF region studied among other regions of the conterminous US for determining the influence of

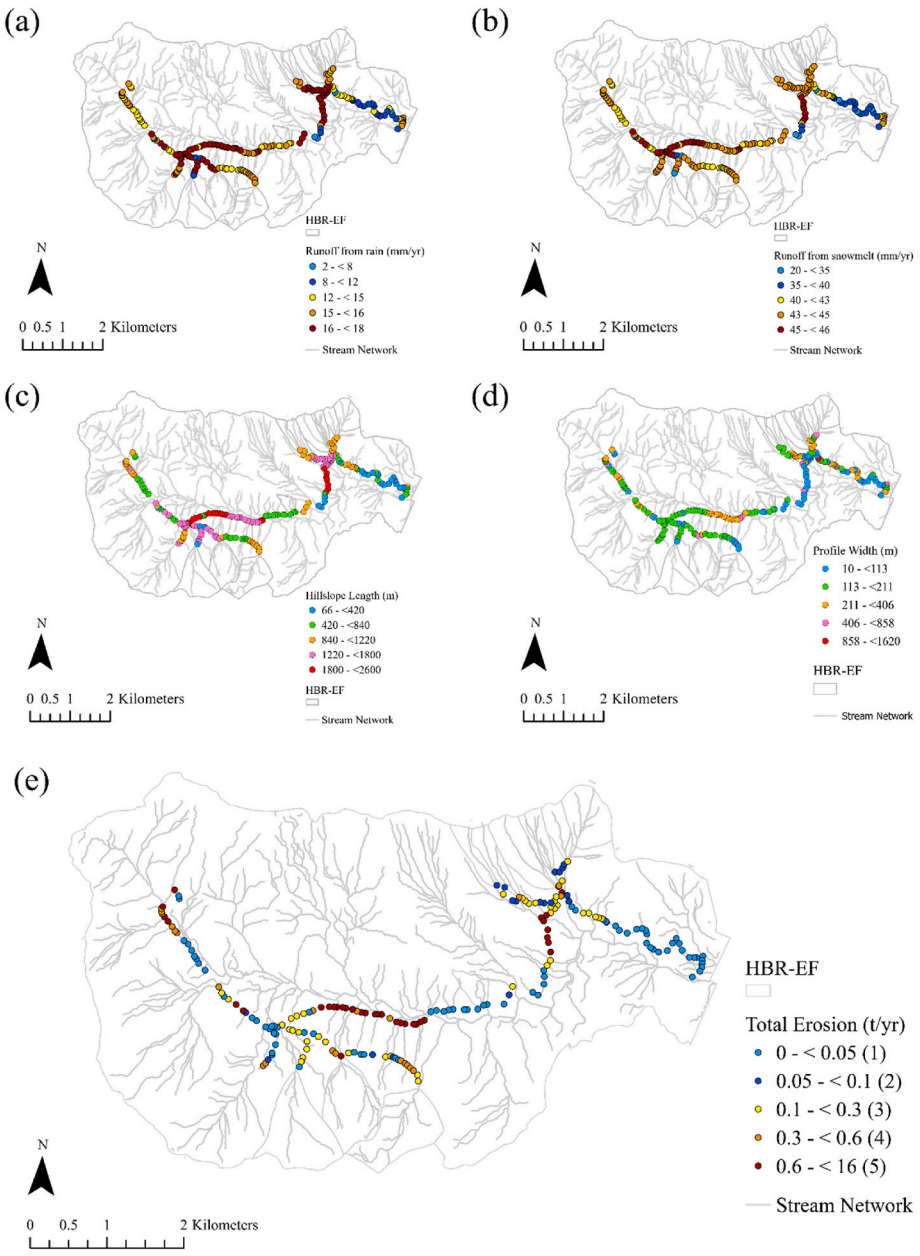

Fig. 6. Spatial maps showing the (a) runoff from rain, (b) runoff from snowmelt, (c) hillslope length, (d) representative profile width of the hillslopes, and (e) total erosion specific to the culverts. Note that in (e), the vulnerability classes are shown in parenthesis.

Table 3
Percentage bias of the average annual erosion rates from 1980 to 2022, as predicted by the WEPP model, compared to the observed average annual erosion rates available for culverts/weirs draining watershed WS1, WS5, and WS6.

Watershed	Average Erosion rate (kg/ha/yr), period 1980–2022		Bias (%)
	Observed	Modeled	
WS1	38	33	−13
WS5	34	52	53
WS6	14.4	30	108

vegetation on soil erosion potential. The erosion rates are dominated by the LS factors due to the complex topography and steep slopes of the headwater catchments, and R factor mainly in the western side of the HBR-EF that experiences greater rainfall due to the aspect and higher elevation of the watershed. Similar findings were reported by Doetterl et al. (2012) which identified slope steepness (S) and the rainfall-runoff erosivity (R) as the key factors influencing erosion rates across large regions of the US.

The WEPP model simulated a relatively higher average annual runoff due to snowmelt compared to rainfall, which makes important contribution to streamflow at the HBR-EF (Campbell et al., 2010). Model evaluation performance ratings consider a percentage bias of ±55% for sediment to be within the satisfactory limits for systematic quantification of accuracy in watershed erosion simulations (Moriasi et al., 2007). The performance of WEPP in simulating erosion was satisfactory in WS1, and WS5 (i.e., the bias was within 55% of the observed). The higher bias in WS6 may be due to disparities between the location of the hillslope outlet and watershed weir originating from the differences in spatial resolution used to delineate the hillslope in this study (5-m generated by LiDAR) and the pre-defined watershed weir locations generated stereophoto-grammetrically based on May 1956 aerial photography (see https://portal.edirepository.org/nis/metadataviewer?packageid=knb-lter-hbr.107.3).

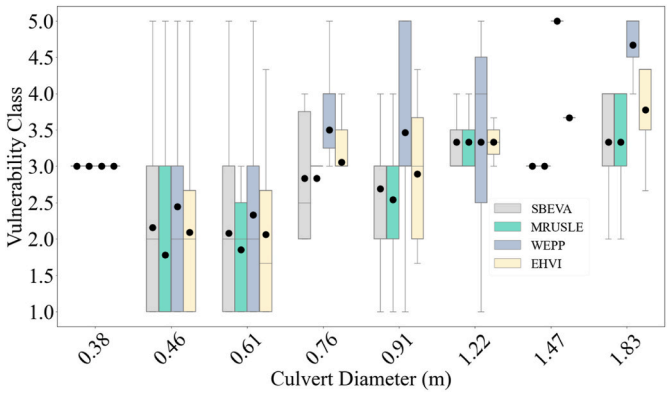

Fig. 7. Boxplots showing the distribution of vulnerability class for given culvert diameters based on SBEVA, MRUSLE, and WEPP model outputs, and EHVI magnitudes. Note that the mean and median values are indicated by black circle and line respectively, and a single horizontal line (indicating median) and the mean values (indicated by black circle) are displayed for culvert diameter of 0.38, 0.76 and 1.47 m because there is only one culvert for each of these classes.

The estimated amount of soil erosion from the forested lands that reaches water bodies is a small fraction of the total loss and depends heavily on factors like stream connectivity (Hamel et al., 2017). The total erosion at the inlet of the culverts from the upstream becomes increasingly sensitive to the drainage area. The increasing disparity between conceptual MRUSLE and process based WEPP simulated total erosion with increasing drainage area demonstrated in the study, corroborates the need for ensemble modeling approach in soil erosion modeling. Disparities between MRUSLE and WEPP model outputs have been reported in previous studies (Renard et al., 1994; Tiwari et al., 2000; Reyes et al., 2004). The WEPP simulated total erosion show higher sensitivity to drainage area compared to MRUSLE, which might be due to disparities in methodology, data used, and the spatial scale at which the two models were applied. While a single event based 30-min 100-yr PI was used in the MRSULE for each 5-m pixel, an event-by-event continuous and hillslope process driven approach using observed storm data for 44-years was implemented in the WEPP simulation. Given that the precipitation data used in these models come from two different sources and some of the storms in the 44-yr period fed into the WEPP model may be more intense than a fixed 30-min 100-yr PI (used in MRUSLE), the output of erosion rates may differ significantly among the models. Given that the success of a vulnerability assessment depends on the balance between factor of safety and restoration cost optimization capabilities (Wear et al., 2013; Piratla et al., 2016), it is more appropriate to rely on the ensemble outputs from SBEVA, WEPP, and MRSULE rather than relying solely on one of them.

It is important to note that while the EHVI proposed in this study accounts for various hydroclimatic and morphological factors, however, it does not factor in the culvert diameter or capacity. Therefore, forest engineers and land managers should recognize that a larger culvert, despite a high EHVI magnitude, can handle greater sediment loads, impacting its actual vulnerability. The EHVI values revealed that hillslope areas draining into larger diameter culverts ($\geq$0.76 m) generally exhibited higher mean EHVI values ($>$3), due to larger upstream hillslope areas exporting larger volume of sediment. However, it is concerning that 7.7 % of culverts with a diameter of 0.46 m, and 1.5 % of culverts with a diameter of 0.61 m show EHVI values 3–4; and 2.6% of culverts with a diameter of 0.46 m and 0.5% of culverts with a diameter of 0.61 m show EHVI values 4–5, indicating their vulnerability to sedimentation caused by erosion, in addition to their hydrological vulnerability to floods causing overtopping in the HBR-EF as reported by Mukherjee et al. (2024). The EHVI strongly correlates with 25-year, 50-year, and 100-year return values of observed annual total soil erosion rates and peak flow, indicating its ability to predict potential erosion rates in HBR-EF. The qualitative evaluation, through a field validation survey, further supported the performance of EHVI. It accurately identified vulnerable culverts with a high accuracy. Nevertheless, the modeling assessment results demonstrated in this study warrant actions for prioritizing these culverts for more rigorous site inspection across a greater number of culvert samples to make a management decision on their restoration based on their hydro-geomorphologic conditions and stability. While the current study provides a strong foundation for its use and evaluation at the HBR-EF, additional factors may need to be considered when applying it to other regions. Specifically, a ground inspection or survey should be performed across at least a random sample of culverts as done in this study, to ascertain the validity of the EHVI to different forest types, culvert samples and characteristics, and hydrological conditions. This will help ensure that the index can be effectively used by researchers and practitioners in various settings.

The SBEVA, MRUSLE, and WEPP models have some limitations in that they do not account for channel scouring, vorticity, or turbulent velocity, which can also significantly impact streambank erosion. While the existing SBEVA methodology only considers upstream sediment deposition, the immediate downstream deposition footprint may also be important for assessing the hydro-geomorphological vulnerability of culverts. This downstream deposition is significantly influenced by local hydraulics including culvert outlet, bank-full width, channel roughness, alignment and bed slope and bank curvature, all of which play a crucial role in the overall sedimentation dynamics near the culvert (Singley and Hotchkiss, 2010; Rees et al., 2018; Xu et al., 2019), potentially resulting in backflow/overtopping in some cases. In general, after upstream sediment accumulates, the deposition footprint typically expands both horizontally and vertically downstream, eventually reaching a “stable” form as a “sediment island” downstream. By incorporating this downstream deposition phenomenon into the assessment, a further advanced SBEVA model can provide a more comprehensive understanding of the streambank vulnerability (Xu et al., 2019; Panda et al., 2022). Soil data, especially, the soil erodibility factor was obtained from SSURGO databases, which have uncertainties stemming from the scale at which the data are collected, potential inconsistencies spatially, and the inclusion of map units that encompass a variable number of unidentified soil components (Ramcharan et al., 2018). Further research that incorporates field-based measurements of soil erodibility for a greater number of watersheds and other soil components at a finer spatial scale could improve the accuracy of our findings. For practical management and culvert design, further research including field validation is needed to understand these complexities, including structural vulnerabilities (Rees et al., 2018). Additionally, WEPP does not account for erosion from permanent gullies, which may not be a concern in undisturbed forested landscapes. Furthermore, the WEPP model has primarily been developed for and applied to watersheds in the Western US, which are characterized by coniferous forests. In contrast, the HBR-EF watershed consists of a mixture of both deciduous and coniferous forests. Lastly, the model has been applied without any calibration, similar to how land managers/engineers might use the model. Despite these limitations, WEPP remains a valuable tool for erosion prediction, but careful consideration should be given when applying it to new environments including the geomorphological vulnerability analysis of culverts in this study.

5. Conclusion

In this study we implemented a hillslope scale ensemble modeling approach using the empirical SBEVA, conceptual MRUSLE and process-based WEPP models to provide a comprehensive hydro-geomorphologic vulnerability assessment at 5-m spatial resolution by assessing the flood-induced soil erosion rates and vulnerability of 194 road-culverts within USDA-FS managed HBR-EF. The goal of the study was to calculate an ensemble hydro-geomorphologic vulnerability index (EHVI) for

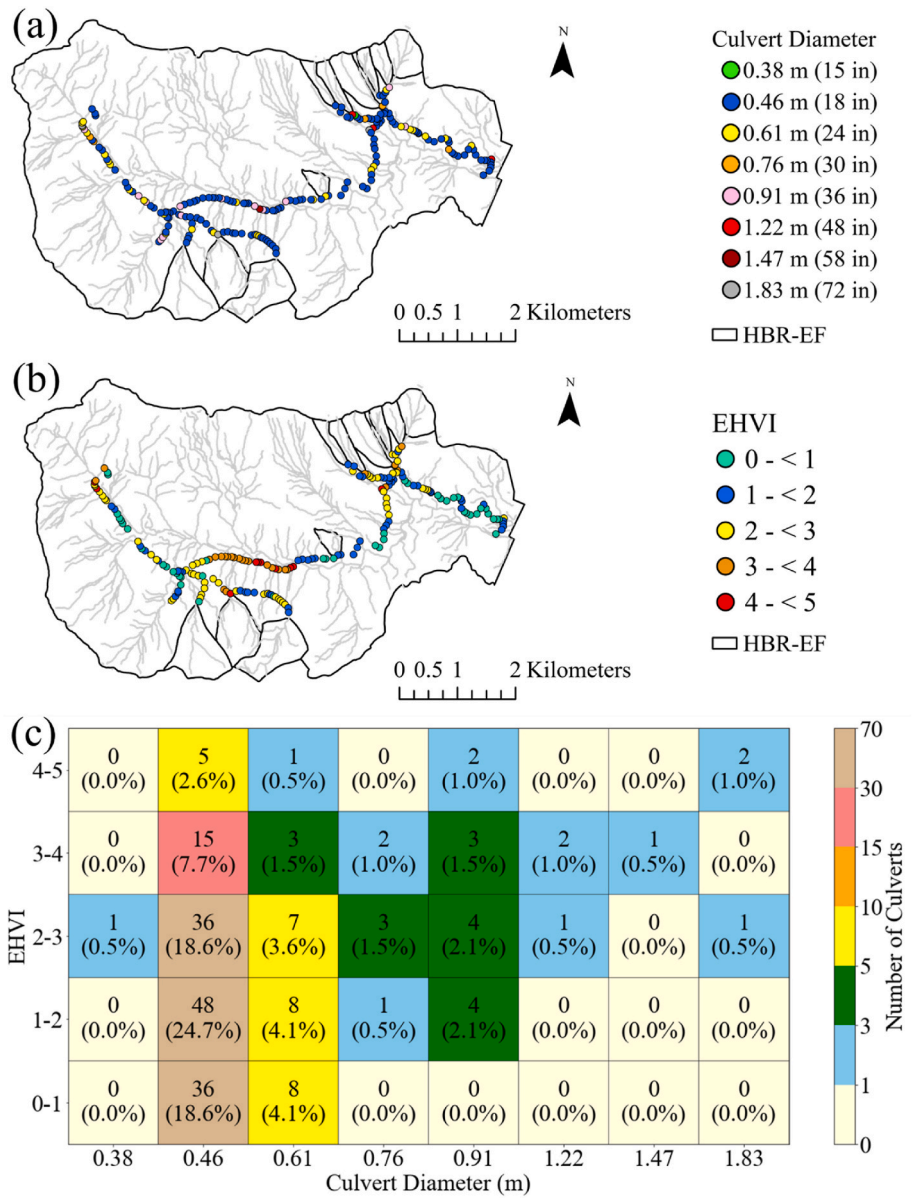

Fig. 8. (a–b) Spatial map showing the (a) culvert diameter (b) EHVI magnitude for each culvert, and (c) heatmap showing the counts (and percentage shown in parenthesis) out of 194 culverts for given culvert diameter and corresponding EHVI range.

identifying culverts that are susceptible to sedimentation and clogging due to soil erosion to inform management and restoration decisions. The ensemble approach successfully integrated event-specific (100-yr 24-hr storm intensity in empirical SBEVA, and 100-yr 30-min storm intensity in conceptual MRUSLE) as well as climate driven continuous hillslope process-based technique in WEPP and evaluated the topographic, hydrologic, morphometric, climatic, and environmental characteristics to identify potentially at-risk culverts at the HBR-EF.

Our ensemble modeling approach is useful not only for making management decisions on culvert vulnerability, but also the findings can be used to develop improved land-use policies that promote soil conservation within the region. This modeling approach uses publicly available datasets and widely used methodologies which makes the EHVI metric easily transferrable to other forests and stream crossings. While the EHVI may be dependent upon the characteristics of the sample of culverts it is being used for, ground inspection of a sample of culverts can be useful to validate the reliability of EHVI when applied to other forest regions. **Additionally, the results can inform the land managers and engineers about strategic investments in restoration, redesign, and installation of road-stream crossings including the culverts. Improvements in the RSCS will enhance flood resilience, potentially reducing economic and societal costs by reducing culvert failure rates and maintenance costs, while safeguarding the critical ecological values including aquatic organism passage in forested watersheds.** It should be noted that there are additional factors that need to be considered by forest managers, field engineers and ecologist before making decisions on culvert restoration for aquatic passage. Two such crucial factors may be (i) beavers and the presence/absence of beaver protection for USFS culverts, and (ii) the impacts of culverts on aquatic habitat connectivity for migratory fish and other organisms, such as culverts that are not clogged but have too high a drop/fall or water velocity for organisms to pass upstream (Jackson, 2003; Gillespie et al., 2014).

It is crucial to emphasize that engineers should meticulously select the most suitable design strategy for new and renovated roads and their infrastructure. This selection should also consider established government criteria (USDOT, 2012; Rasmussen et al., 2018) and sound engineering judgement specific to the watershed

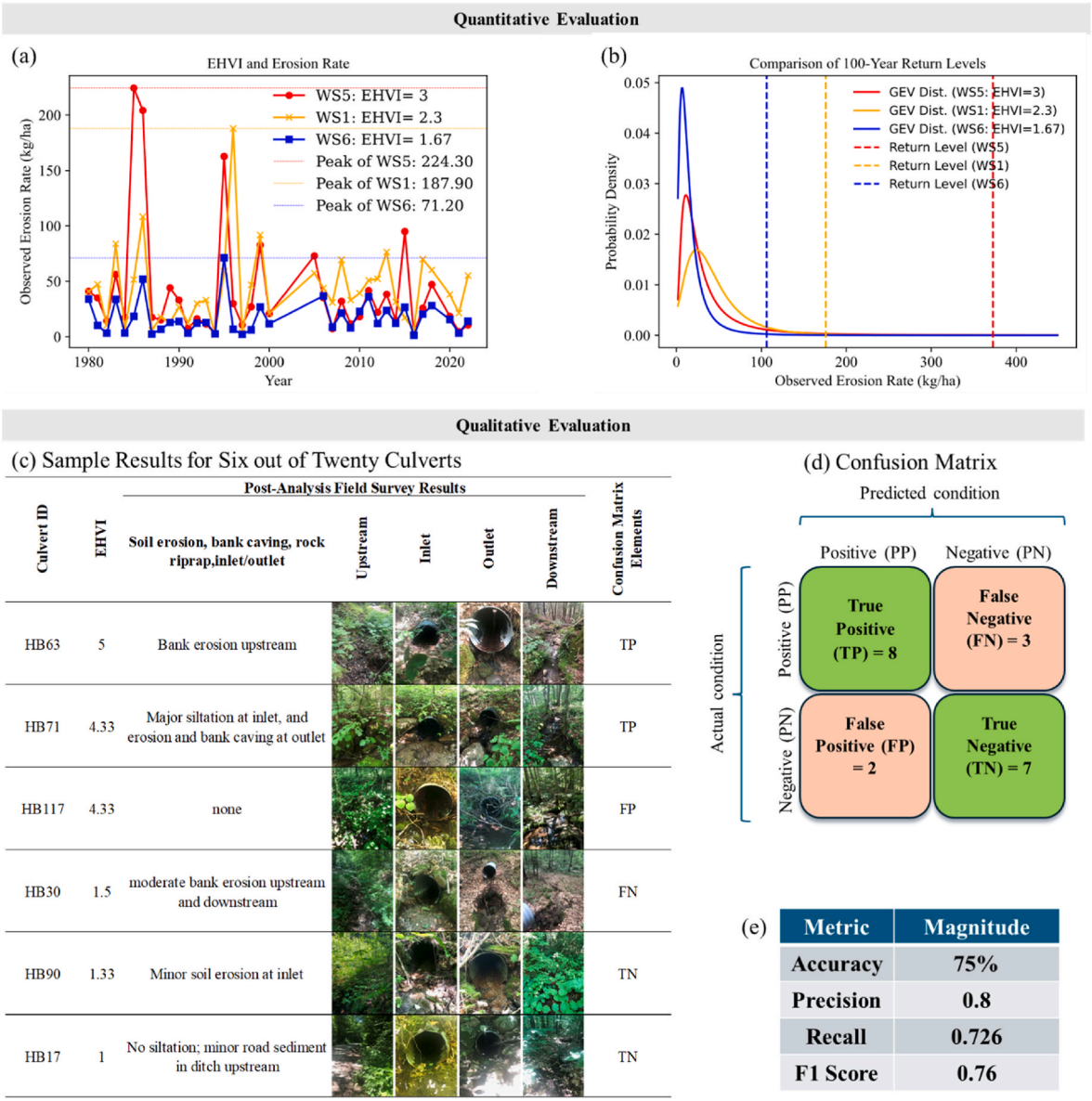

Fig. 9. (a–b) Results of quantitative evaluation of EHVI showing (a) annual variation of observed erosion rates (in kg/ha) and their peak values over the period 1980–2022, and (b) probability density functions and 100-yr return values of the observed erosion rates for culverts (or weirs) draining WS1, WS5, and WS6 and their corresponding EHVI values. Note that the observed erosion data were recorded at irregular intervals. Therefore, the starting year of the records were assumed to be the year of the record as represented in the x-axis of (a), and (c–e) qualitative evaluation of EHVI showing the (c) the results of post-analysis field validation survey for six out of the twenty culverts and their corresponding confusion matrix elements, (d) the confusion matrix and its elements, and (e) the evaluation metrics, including accuracy and F1 score.

and culverts in question. Following design completion, careful consideration should also be given to the proposed culvert installation procedures, including alignment checks, stream dimension verification for bank-full discharge, and substrate composition evaluation (Hansen et al., 2009; Gillespie et al., 2014). Finally, future application of SBEVA, RUSLE, and WEPP models, with some appropriate modifications using more nuanced techniques of probable maximum precipitation estimation (NAS, 2024), could further improve post-wildfire erosion and debris flow modeling in similar other forest landscapes, especially in the western US where post-wildfire flooding has significant, long-lasting impacts on ecological, social, and economic systems (Scott et al., 2013; Beyene et al., 2021).

Disclaimer

The opinions presented in this article are those of the authors and should not be construed to represent any official USDA or US Government determination or policy.

CRediT authorship contribution statement

Sourav Mukherjee: Writing – original draft, Visualization, Validation, Software, Resources, Methodology, Investigation, Formal analysis, Data curation, Conceptualization. **Sudhanshu Panda:** Writing – review & editing, Supervision, Software, Methodology, Funding acquisition, Conceptualization. **Devendra M. Amatya:** Writing – review & editing, Supervision, Resources, Project administration, Funding acquisition, Conceptualization. **Mariana Dobre:** Writing – review & editing, Supervision, Methodology, Conceptualization. **John L. Campbell:** Writing – review & editing, Resources. **Roger Lew:** Software. **Peter Caldwell:** Writing – review & editing. **Kelly Elder:** Writing – review & editing. **Johnny M. Grace:** Writing – review & editing. **Sherri L. Johnson:**

Writing – review & editing.

Declaration of competing interest

The authors declare that they have no known competing financial interests or personal relationships that could have appeared to influence the work reported in this paper.

Acknowledgements

This work is primarily funded by US Department of Transportation Federal Highway Administration's Innovative Research Council in support of the "23ASM004 Developing an Automated Geospatial Model-based Decision Support Tool for Assessing Road Culvert Vulnerability on USDA Forest Service Experimental Forests" project. This work is also supported by funding agreements (#22JV11330180-063 and #24-CR-11330180-001) between the USDA Forest Service Southern Research Station and The University of North Georgia and also another funding agreement (#23-IA-11330180-042) with the Oak Ridge Institute for Science and Education (ORISE). We are thankful for the climate, and soil erosion data provided by USDAFS researchers, Dr. Nina Lany at the Hubbard Brook EF, USGS, SSURGO, and NOAA. We thank technicians, Ian Halm, Hannah Vollmer, Garrett Higgins, and Gabe Winant for providing the culvert dataset for the Hubbard Brook EF. We gratefully acknowledge the help of Shawna Reid at the USDAFS Southern Research Station, for acquiring the geospatial dataset of watersheds and related information about road-stream crossings and road networks located across the EFs in this study. We also acknowledge USDA's National Agriculture Imagery Program for the LULC data (https://datagateway.nrcs.usda.gov/); USDA Natural Resources Conservation Service Geospatial Data Gateway for the elevation data available at https://datagateway.nrcs.usda.gov/; Census Bureau's Topologically Integrated Geographic Encoding and Referencing (TIGER) database (https://datagateway.nrcs.usda.gov/), Enterprise Data Warehouse of the US Forest Service (https://www.fs.usda.gov/about-agency/enterprise-data-warehouse), and US Transit Roads (https://www.bts.gov/maps); NOAA for Atlas-14's precipitation frequency data services (https://hdsc.nws.noaa.gov/hdsc/pfds/); PRISM climate group for PRISM data (https://prism.oregonstate.edu/normals/) and University of Idaho for gridMET data (https://developers.google.com/earth-engine/datasets/catalog/IDAHO_EPSCOR_GRIDMET); and USDA and NRCS for SSURGO data (https://websoilsurvey.nrcs.usda.gov/app/).

Appendix A. Supplementary data

Supplementary data to this article can be found online at https://doi.org/10.1016/j.envsoft.2024.106243.

Data availability

Data will be made available on request.

References

Abatzoglou, J.T., 2013. Development of gridded surface meteorological data for ecological applications and modelling. Int. J. Climatol. 33 (1), 121–131.

Aksoy, H., Kavvas, M.L., 2005. A review of hillslope and watershed scale erosion and sediment transport models. Catena 64 (2–3), 247–271.

Amatya, D.M., Campbell, J., Wohlgemuth, P., Elder, K., Sebestyen, S., Johnson, S., Keppeler, E., Adams, M.B., Caldwell, P., Misra, D., 2016. Hydrological processes of reference watersheds in experimental forests, USA. Forest hydrology: Processes, management and assessment. Cabi, Wallingford UK, pp. 219–239.

Amatya, D.M., Tian, S., Marion, D.A., Caldwell, P., Laseter, S., Youssef, M.A., Grace, J.M., Chescheir, G.M., Panda, S., Ouyang, Y., Sun, G., 2021. Estimates of precipitation IDF curves and design discharges for road-crossing drainage structures: case study in four small forested watersheds in the Southeastern US. J. Hydrol. Eng. 26 (4), 05021004.

Bagwan, W.A., Gavali, R.S., 2021. Delineating changes in soil erosion risk zones using RUSLE model based on confusion matrix for the Urmodi river watershed, Maharashtra, India. Modeling Earth Systems and Environment 7 (3), 2113–2126.

Beilicci, E.B., Beilicci, R.F., 2024. Flash floods: causes, effects, and modeling possibilities with advanced hydroinformatic tools. In: Modeling and Monitoring Extreme Hydrometeorological Events. IGI Global, City?, pp. 42–69.

Benavidez, R., Jackson, B., Maxwell, D., Norton, K., 2018. A review of the (Revised) Universal Soil Loss Equation ((R) USLE): with a view to increasing its global applicability and improving soil loss estimates. Hydrol. Earth Syst. Sci. 22 (11), 6059–6086.

Benjankar, R., Koenig, F., Tonina, D., 2013. Comparison of hydromorphological assessment methods: application to the boise river, USA. J. Hydrol. 492, 128–138. https://doi.org/10.1016/j.jhydrol.2013.03.017.

Beyene, M.T., Leibowitz, S.G., Pennino, M.J., 2021. Parsing weather variability and wildfire effects on the post-fire changes in daily stream flows: a quantile-based statistical approach and its application. Water Resour. Res. 57, e2020WR028029. https://doi.org/10.1029/2020WR028029.

Borrelli, P., Lugato, E., Montanarella, L., Panagos, P., 2017. A new assessment of soil loss due to wind erosion in European agricultural soils using a quantitative spatially distributed modelling approach. Land Degrad. Dev. 28 (1), 335–344.

Cancienne, R.M., Fox, G.A., Simon, A., 2008. Influence of seepage undercutting on the stability of root-reinforced streambanks. Earth Surface Processes and Landforms. The Journal of the British Geomorphological Research Group 33 (11), 1769–1786.

Campbell, J.L., Rustad, L.E., Bailey, S.W., Bernhardt, E.S., Driscoll, C.T., Green, M.B., Groffman, P.M., Lovett, G.M., McDowell, W.H., McGuire, K.J., Rosi, E.J., 2021. Watershed studies at the Hubbard Brook Experimental Forest: building on a long legacy of research with new approaches and sources of data. Hydrol. Process. 35 (1), e14016.

Campbell, J.L., Ollinger, S.V., Flerchinger, G.N., Wicklein, H., Hayhoe, K., Bailey, A.S., 2010. Past and projected future changes in snowpack and soil frost at the Hubbard Brook Experimental Forest, New Hampshire, USA. Hydrol. Process. 24 (17), 2465–2480.

Coles, S., Bawa, J., Trenner, L., Dorazio, P., 2001. An introduction to statistical modeling of extreme values, Vol. 208. Springer, London, p. 208.

Costabile, P., Cea, L., Barbaro, G., Costanzo, C., Llena, M., Vericat, D., 2024. Evaluation of 2D hydrodynamic-based rainfall/runoff modelling for soil erosion assessment at a seasonal scale. J. Hydrol. 632, 130778.

Daly, C., Taylor, G.H., Gibson, W.P., 1997. The PRISM approach to mapping precipitation and temperature. InProc., 10th AMS Conf. on Applied Climatology. Oct 20, 20–23.

Dobre, M., Srivastava, A., Lew, R., Deval, C., Brooks, E.S., Elliot, W.J., Robichaud, P.R., 2022. WEPPcloud: an online watershed-scale hydrologic modeling tool. Part II. Model performance assessment and applications to forest management and wildfires. J. Hydrol. 610, 127776.

Dun, S., Wu, J.Q., Elliot, W.J., Robichaud, P.R., Flanagan, D.C., Frankenberger, J.R., Brown, R.E., Xu, A.C., 2009. Adapting the water erosion prediction project (WEPP) model for forest applications. J. Hydrol. 366 (1–4), 46–54.

Drobot, S., Parker, D.J., 2007. Advances and challenges in flash flood warnings. Environ. Hazards 7 (3), 173–178.

Doetterl, S., Van Oost, K., Six, J., 2012. Towards constraining the magnitude of global agricultural sediment and soil organic carbon fluxes. Earth Surf Proc Land 37, 642–655. https://doi.org/10.1002/esp.3198.

Flanagan, D.C., Laflen, J.M., 1997. The USDA water erosion prediction project (WEPP). The Rest of Citation?, pp. 600–605.

Foltz, R.B., Yanosek, K.A., Brown, T.M., 2008. Sediment concentration and turbidity changes during culvert removals. J. Environ. Manag. 87 (3), 329–340.

Fox, G.A., Wilson, G.V., 2010. The role of subsurface flow in hillslope and stream bank erosion: a review. Soil Sci. Soc. Am. J. 74 (3), 717–733.

Furniss, M.J., Love, M., Flanagan, S.A., 1997. Diversion potential at road-stream crossings. USDA Forest Service, Technology & Development Program. Dec. should there be a city here?

Furniss, M.J., Ledwith, T.S., Love, M.A., McFadin, B.C., Flanagan, S.A., 1998. Response of Road-Stream Crossings to Large Flood Events in Washington, Oregon, and Northern California. Publication. Sep. should there be a city here?

Flanagan, D.C., Nearing, M.A., 1995. USDA-water erosion prediction project (WEPP): hillslope profile and watershed model documentation, NSERL report 10. US department of agriculture. Agricultural Research Service, National Soil Erosion Research Laboratory. Purdue University, West Lafayette, Indiana, USA.

Flanagan, D.C., Frankenberger, J.R., Cochrane, T.A., Renschler, C.S., Elliot, W.J., 2013. Geospatial application of the water erosion prediction project (WEPP) model. Transactions of the ASABE 56 (2), 591–601.

Foster, G.R., Flanagan, D.C., Nearing, M.A., Lane, L.J., Risse, L.M., Finkner, S.C., 1995. Hillslope erosion component. In: WEPP: USDA-Water Erosion Prediction Project. USDA ARS Lafayette. Vol. 10, pp. 11–1. https://www.ars.usda.gov/ARSUserFiles/50201000/WEPP/chap11.pdf.

EPA US Environmental Protection Agency, 2008. Integrated Modeling for Integrated Environmental Decision MakingOffice of the Science Advisor. Washington, DC. http://www.epa.gov/CREM/library/IM4IEDM_White_Paper_Final_(EPA100R08010). EPA-100-R-08-010.

Fernandez, C., Wu, J.Q., McCool, D.K., Stöckle, C.O., 2003. Estimating water erosion and sediment yield with GIS, RUSLE, and SEDD. Journal of soil and Water Conservation 58 (3), 128–136.

Gillespie, N., Unthank, A., Campbell, L., Anderson, P., Gubernick, R., Weinhold, M., Cenderelli, D., Austin, B., McKinley, D., Wells, S., Rowan, J., Orvis, C., Hudy, M., Bowden, A., Singler, A., Fretz, E., Levine, J., Kirn, R., 2014. Flood effects on road–stream crossing infrastructure: economic and ecological benefits of stream simulation designs. Fisheries 39, 62–76. https://doi.org/10.1080/03632415.2013.874527.

Glasser, S.P., 2005. History of watershed management in the US forest service: 1897–2005. J. For. 103 (5), 255–258.
Goodman, A.C., Segura, C., Jones, J.A., Swanson, F.J., 2023. Seventy years of watershed response to floods and changing forestry practices in western Oregon, USA. Earth Surface Processes and Landforms 48 (6), 1103–1118.
Hamel, P., Falinski, K., Sharp, R., Auerbach, D.A., Sánchez-Canales, M., Dennedy-Frank, P.J., 2017. Sediment delivery modeling in practice: comparing the effects of watershed characteristics and data resolution across hydroclimatic regions. Sci. Total Environ. 580, 1381–1388. https://doi.org/10.1016/j.scitotenv.2016.12.103 [PubMed] [CrossRef] [Google Scholar] [Ref list].
Heredia, N., Roper, B., Gillespie, N., Roghair, C., 2016. Technical guide for field practitioners: understanding and monitoring aquatic organism passage at road-stream crossings. US Department of Agriculture, Forest Service, National Stream and Aquatic Ecology Center. Technical Report TR-101, City?
Hansen, B., Nieber, J.L., Lenhart, C., 2009. Cost Analysis of Alternative Culvert Installation Practices in Minnesota.
Jackson, S.D., 2003. Design and Construction of Aquatic Organism Passage at Road-Stream Crossings: Ecological Considerations in the Design of River and Stream Crossings.
Jakeman, A.J., Letcher, R.A., 2003. Integrated assessment and modelling: features, principles and examples for catchment management. Environmental Modelling & Software 18 (6), 491–501.
Jencso, K.G., McGlynn, B.L., Gooseff, M.N., Wondzell, S.M., Bencala, K.E., Marshall, L.A., 2009. Hydrologic connectivity between landscapes and streams: transferring reach- and plot-scale understanding to the catchment scale. Water Resour. Res. 45 (4).
Keller, G., Sherar, J., 2003. Low-volume Roads Engineering: Best Management Practices Field Guide.
Kuksina, L.V., Golosov, V.N., Kuznetsova, Y.S., 2017. Cloudburst floods in mountains: state of knowledge, occurrence, factors of formation. Geogr. Nat. Resour. 38, 20–29. https://doi.org/10.1134/S1875372817010036.
Langendoen, E.J., Simon, A., 2008. Modeling the evolution of incised streams. II: streambank erosion. J. Hydraul. Eng. 134 (7), 905–915.
Lew, R., Dobre, M., Srivastava, A., Brooks, E.S., Elliot, W.J., Robichaud, P.R., Flanagan, D.C., 2022. WEPPcloud: an online watershed-scale hydrologic modeling tool. Part I. Model description. J. Hydrol. 60, 127603.
Laniak, G.F., Olchin, G., Goodall, J., Voinov, A., Hill, M., Glynn, P., Whelan, G., Geller, G., Quinn, N., Blind, M., Peckham, S., 2013. Integrated environmental modeling: a vision and roadmap for the future. Environmental modelling & software 39, 3–23.
Lew, R., 2024. Wepp-In-The-Woods/Peridot: Release 1.0 (Release). Zenodo. https://doi.org/10.5281/zenodo.13655432.
Laflen, J.M., Lane, L.J., Foster, G.R., 1991. WEPP: a new generation of erosion prediction technology. J. Soil Water Conserv. 46 (1), 34–38.
Laflen, J.M., Elliot, W.J., Flanagan, D.C., Meyer, C.R., Nearing, M.A., 1997. WEPP–Predicting water erosion using a process-based model. J. Soil Water Conserv. 52, 96–102. https://www.jswconline.org/content/52/2/96.short.
Martin, C.W., Hornbeck, J.W., 1994. Logging in new england need not cause sedimentation of streams. N. J. Appl. For. 11 (1), 17–23.
Marx, R.W., 1990. The TIGER system: automating the geographic structure of the United States Census. In: Peuquet, Donna J., Francis Marble, Duane (Eds.), Introductory Readings in Geographic Information Systems. CRC Press. ISBN 0-85066-857-3.
Massey Jr., F.J., 1951. The Kolmogorov-Smirnov test for goodness of fit. J. Am. Stat. Assoc. 46 (253), 68–78.
McEachran, Z.P., Karwan, D.L., Slesak, R.A., 2021. Direct and indirect effects of forest harvesting on sediment yield in forested watersheds of the United States. J. Am. Water Resour. Assoc. 57 (1), 1–31.
Moriasi, D.N., Arnold, J.G., Van Liew, M.W., Bingner, R.L., Harmel, R.D., Veith, T.L., 2007. Model evaluation guidelines for systematic quantification of accuracy in watershed simulations. Transactions of the ASABE 50 (3), 885–900.
Mukherjee, S., 2024. Automated data pipeline for batch pre-processing, post-processing, and running water erosion prediction project (WEPP) model simulation using Python [Software], Version 1.0. https://github.com/SouravDSGit/WEPP_model_run/new/main.
Mukherjee, S., Amatya, D.M., Campbell, J.L., Gryczkowski, L., Panda, S., Johnson, S.L., Elder, K., Jalowska, A.M., Caldwell, P., Grace, J.M., Młyński, D., 2024. A watershed-scale multi-approach assessment of design flood discharge estimates used in hydrologic risk analyses for forest road stream crossings and culverts. J. Hydrol. 632, 130698.
Mukherjee, S., Amatya, D.M., Jalowska, A.M., Campbell, J.L., Johnson, S.L., Elder, K., Panda, S., Grace, J.M., Kikoyo, D., 2023. Comparison of on-site versus NOAA's extreme precipitation intensity-duration-frequency estimates for six forest headwater catchments across the continental United States. Stoch. Environ. Res. Risk Assess. 37 (10), 4051–4070.
Mishra, A., Mukherjee, S., Merz, B., Singh, V.P., Wright, D.B., Villarini, G., Paul, S., Kumar, D.N., Khedun, C.P., Niyogi, D., Schumann, G., 2022. An overview of flood concepts, challenges, and future directions. J. Hydrol. Eng. 27 (6), 03122001.
MacMillan, D.C., Marshall, K., 2006. The Delphi process – an expert-based approach to ecological modelling in data-poor environments. Anim. Conserv. 9, 11–19. https://doi.org/10.1111/j.1469-1795.2005.00001.x.
MacDonald, L.H., Coe, D.B., 2008. Road Sediment Production and Delivery: Processes and Management. InProceedings of the First World Landslide Forum, International Programme on Landslides and International Strategy for Disaster Reduction Nov 18. United Nations University, Tokyo, Japan, pp. 381–384.
Muste, M., Xu, H., 2022. Multi-pronged approach for monitoring sedimentation processes at multi-barrel culverts. J. Hydrol. 610, 127840.
Naipal, V., Ciais, P., Wang, Y., Lauerwald, R., Guenet, B., Van Oost, K., 2018. Global soil organic carbon removal by water erosion under climate change and land use change during AD 1850–2005. Biogeosciences 15 (14), 4459–4480.
National Academies of Sciences, Engineering, and Medicine, 2024. Modernizing Probable Maximum Precipitation Estimation. The National Academies Press, Washington, DC. https://doi.org/10.17226/27460.
Nearing, M.A., Foster, G.R., Lane, L.J., Finkner, S.C., 1989. A process-based soil erosion model for USDA-Water Erosion Prediction Project technology. Transactions of the ASAE 32 (5), 1587–1593.
Panda, S.S., Andrianasolo, H., Steele, D.D., 2005. Application of geotechnology to watershed soil conservation planning at the field scale. J. Environ. Hydrol. 13.
NRCS, U., 2020. America's Private Land: A Geography of Hope. United States Department of Agriculture–Natural Resources Conservation Service, Washington, DC, p. 39.
Panda, S.S., 2024. ArcGIS toolbox for modified revised soil loss equation and streambank erosion vulnerability assessment model (version 1.0) [Software]. https://github.com/SouravDSGit/MRUSLE_SBEVA/new/main.
Panda, S.S., Misra, D., Amatya, D., Thompson, A., Grace, J., 2024. Soil erosion model modification and subsequent soil conservation decision support system development with climate change – a Chapter (#7) in the Book. In: Seeger, K.M.B.D.S. (Ed.), Understanding and Preventing Soil Erosion. Publishing, Cambridge, UK (*In Print*).
Panda, S.S., Amatya, D.M., Grace, J.M., Caldwell, P., Marion, D.A., 2022. Extreme precipitation-based vulnerability assessment of road-crossing drainage structures in forested watersheds using an integrated environmental modeling approach. Environ. Model. Software 155, 105413.
Pandey, A., Himanshu, S.K., Mishra, S.K., Singh, V.P., 2016. Physically based soil erosion and sediment yield models revisited. Catena 147, 595–620.
Piratla, K.R., Pang, W., Jin, H., Stoner, M., 2016. Best Practices for Assessing Culvert Health and Determining Appropriate Rehabilitation Methods: a Research Project in Support of Operational Requirements for the South Carolina Department of Transportation. South Carolina. Dept. Of Transportation. Office of Materials and Research. Nov 1.
Parker, P., Letcher, R., Jakeman, A., Beck, M.B., Harris, G., Argent, R.M., Hare, M., Pahl-Wostl, C., Voinov, A., Janssen, M., Sullivan, P., 2002. Progress in integrated assessment and modelling. Environmental Modelling & Software 17 (3), 209–217.
Perica, S., Pavlovic, S., St Laurent, M., Trypaluk, C., Unruh, D., Martin, D., Wilhite, O., 2015. Precipitation-frequency Atlas of the United States. In: Northern States; Connecticut, Maine, Massachusetts, New Hampshire, New York, Rhode Island, Vermont, ume 10, Version 3.0.
Poesen, J., Nachtergaele, J., Verstraeten, G., Valentin, C., 2003. Gully erosion and environmental change: importance and research needs. Catena 50 (2–4), 91–133.
Raj, R., Saharia, M., Chakma, S., 2024. Geospatial modeling and mapping of soil erosion in India. Catena 240, 107996.
Ramcharan, A., Hengl, T., Nauman, T., Brungard, C., Waltman, S., Wills, S., Thompson, J., 2018. Soil property and class maps of the conterminous United States at 100-meter spatial resolution. Soil Sci. Soc. Am. J. 82 (1), 186–201.
Rasmussen, B., Lamoureux, K., Simmons, E., Miller, R., 2018. *US Forest Service Transportation Resiliency Guidebook: Addressing Climate Change Impacts on*. US Forest Service Transportation Assets (No. DOT-VNTSC-USDA-19-01). United States. Forest Service.
Rees, P.L., Jackson, S.D., Mabee, S.B., Mcarthur, K.M., 2018. A Proposed Method for Assessing the Vulnerability of Road-Stream Crossings to Climate Change: Deerfield River Watershed Pilot. University of Massachusetts, Amherst, MA.
Renard, K.G., Laflen, J.M., Foster, G.R., McCool, D.K., 2017. The revised universal soil loss equation. Soil erosion research methods Oct 19, 105–126. Routledge.
Renard, K.G., Foster, G.R., Yoder, D.C., McCool, D.K., 1994. RUSLE revisited: status, questions, answers, and the future. J. Soil Water Conserv. 49 (3), 213–220.
Renard, K.G., 1997. Predicting soil erosion by water: a guide to conservation planning with the Revised Universal Soil Loss Equation (RUSLE). Agricultural Research Service. US Department of Agriculture.
Renschler, C.S., 2003. Designing geo-spatial interfaces to scale process models: the GeoWEPP approach. Hydrol. Process. 17 (5), 1005–1017.
Risse, L.M., Nearing, M.A., Laflen, J.M., Nicks, A.D., 1993. Error assessment in the universal soil loss equation. Soil Sci. Soc. Am. J. 57 (3), 825–833.
Reyes, M.R., Raczkowski, C.W., Gayle, G.A., Reddy, G.B., 2004. Comparing the soil loss predictions of GLEAMS, RUSLE, EPIC, and WEPP. Transactions of the ASAE 47 (2), 489–493.
EPA, U., 2000. *Atlas of America's polluted waters*. EPA 840-B00-002. Washington DC.
Scott, J.H., Thompson, M.P., Calkin, D.E., 2013. A wildfire risk assessment framework for land and resource management. Gen. Tech. Rep. RMRS-GTR-315. U.S. Department of Agriculture, Forest Service, Rocky Mountain Research Station, p. 83.
Seddon, N., Smith, A., Smith, P., Key, I., Chausson, A., Girardin, C., House, J., Srivastava, S., Turner, B., 2021. Getting the message right on nature-based solutions to climate change. Global Change Biol. 27 (8), 1518–1546.
Shi, W., Chen, T., Yang, J., Lou, Q., Liu, M., 2022. An improved MUSLE model incorporating the estimated runoff and peak discharge predicted sediment yield at the watershed scale on the Chinese Loess Plateau. J. Hydrol. 614, 128598.
Shields Jr., F.D., Bowie, A.J., Cooper, C.M., 1995. Control of streambank erosion due to bed degradation with vegetation and structure 1. J. Am. Water Resour. Assoc. 31 (3), 475–489.
Singley, B.C., Hotchkiss, R.H., 2010. Differences between open-channel and culvert hydraulics: implications for design. InWorld Environmental and Water Resources Congress 2010: Challenges of Change, pp. 1278–1287.
Srivastava, A., Flanagan, D.C., Frankenberger, J.R., Engel, B.A., 2019. Updated climate database and impacts on WEPP model predictions. J. Soil Water Conserv. 74 (4), 334–349.

Tsegaye, L., Bharti, R., 2021. Soil erosion and sediment yield assessment using RUSLE and GIS-based approach in Anjeb watershed, Northwest Ethiopia. SN Appl. Sci. 3, 582. https://doi.org/10.1007/s42452-021-04564-x.

Tiwari, A.K., Risse, L.M., Nearing, M.A., 2000. Evaluation of WEPP and its comparison with USLE and RUSLE. Transactions of the ASAE 43 (5), 1129–1135.

Truhlar, A.M., Marjerison, R.D., Gold, D.F., Watkins, L., Archibald, J.A., Lung, M.E., Meyer, A., Walter, M.T., 2020. Rapid remote assessment of culvert flooding risk. Journal of Sustainable Water in the Built Environment 6 (2), 06020001.

USDA Forest Service, Northern Research Station, 2024. Hubbard Brook Experimental Forest: Sediment Yield in Weir Basins, 1956 - Ongoing Ver 7. Environmental Data Initiative. https://doi.org/10.6073/pasta/141593a14e6d9308dbecbd75d6b481ab.

USDOT, 2012. Evaluating scour at bridges. Hydraulic Engineering Circular No. 18, Publication No. FHWA-HIF-12-003. Federal Highway Administration, Washington, DC. USDOT.

Van der Knijff, J.M., Jones, R.J.A., Montanarella, L., 2000. Soil Erosion Risk Assessment in Europe, 34. European Commission, European Soil Bureau.

Wilson, C.G., Schilling, K.E., Papanicolaou, T., 2022. Evaluating causal factors that influence the spatial and temporal variability of streambank erosion in Iowa. Journal of the ASABE. 65 (6), 1465–1473.

Woznicki, S.A., Cada, P., Wickham, J., Schmidt, M., Baynes, J., Mehaffey, M., Neale, A., 2020. Sediment retention by natural landscapes in the conterminous United States. Sci. Total Environ. 745, 140972.

Wear, L.R., Aust, W.M., Bolding, M.C., Strahm, B.D., Dolloff, C.A., 2013. Effectiveness of best management practices for sediment reduction at operational forest stream crossings. For. Ecol. Manag. 289, 551–561.

Wischmeier, W.H., Smith, D.D., 1978. Predicting Rainfall Erosion Losses: a Guide to Conservation Planning. Department of Agriculture, Science and Education Administration, City?

Xu, H., Muste, M., Demir, I., 2019. Web-based geospatial platform for the analysis and forecasting of sedimentation at culverts. J. Hydroinf. 21 (6), 1064–1081.

Yin, S., Nearing, M.A., Borrelli, P., Xue, X., 2017. Rainfall erosivity: an overview of methodologies and applications. Vadose Zone J. 16 (12), 1–6.

Cafferata, P., Cafferata, P.H., 2004. Designing Watercourse Crossings for Passage of 100 Year Flood Flows, Wood, and Sediment. California Department of Forestry and Fire Protection, Sacramento, CA, USA.